THE JOURNAL OF COMPARATIVE NEUROLOGY 194:663-701 (1980)

The Thalamocortical and Corticothalamic Connections of AI, AII, and the Anterior Auditory Field (AAF) in the Cat: Evidence for Two Largely Segregated Systems of Connections

RICHARD A. ANDERSEN, PAUL L. KNIGHT, AND MICHAEL M. MERZENICH
Departments of Physiology and Otolaryngology, Coleman Laboratory-863 HSE, University of California, San Francisco, California 94143

ABSTRACT The thalamocortical and corticothalamic connections of the three cortical auditory fields—first (AI), second (AII), and anterior (AAF)—were defined using anterograde and retrograde tracing techniques. Microinjections of tracers were placed at one or two different physiologically identified loci after these fields had been mapped using microelectrode recording techniques. This approach ensured that the injections were well within the borders of each field that was studied. By making injections at different positions in the cochleotopic representations in AI and AAF the systematic topographies of the connections between these cortical fields and the medial geniculate body subdivisions were determined.

The thalamocortical and corticothalamic reciprocal projections of single loci in AI were from and to single columns passing rostrocaudally through the deep dorsal nucleus (Dd) and medial division (M) of the medial geniculate body (MGB) and from and to folded sheets of labelled neurons passing rostrocaudally through pars lateralis (Vl) and pars ovoidea (Vo) of the ventral division. The connections of AI with Vl and Vo were very strong. There were also thalamocortical and corticothalamic connections between the lateral division of the posterior group of thalamus (POl) and single loci in AI.

The thalamocortical and corticothalamic reciprocal connections of AAF with the auditory thalamus were similar to the AI connections with the exception that the connections with the ventral division of the MGB were relatively weaker and, in the case of the thalamocortical projection, more discontinuous.

AII loci are thalamocortically and corticothalamically connected with the caudal dorsal nucleus (Dc), the ventral lateral nucleus (VL), and the medial division (M).

The topography of all connections of AAF and AI with the MGB varied systematically and was consistent with a cochleotopic organization of connections between the MGB and the two cortical fields.

Since the thalamocortical and corticothalamic connections of these three cortical fields are reciprocal, we were able to compare directly their connections in individual cats by introducing anterograde tracer in one field and retrograde tracer in another. While AI and AAF were connected to the same subdivisions of the MGB and had the same systematic topography of connections, the connections of AII and AI (or AAF) were largely segregated (with the only

Correspondence to: Richard A. Andersen, Department of Physiology, The Johns Hopkins University, School of Medicine, 725 N. Wolfe St., Baltimore, MD 21205.

0021-9967/80/1943-0663$06.50

overlap occurring in M). Results of injections introduced into other cortical fields in this study and the results of previous studies by other investigators (Rose and Woolsey, '58; Graybiel, '73; Casseday et al., '76; Winer et al., '77) are consistent with the interpretation that there are two largely segregated connectional systems between the auditory thalamus and cortex: a "cochleotopic system" that includes AI and AAF and a "diffuse system" that includes AII.

Small injections of anterograde tracers at higher-frequency representational sites in AI or AAF, or of retrograde tracer in AI, produced a discontinuous, periodic pattern of dense and light labelling in Vl. Reconstructions showed that these discontinuities of label, in three dimensions, formed parallel columns oriented rostrocaudally.

The auditory neuroaxis is remarkable in its structural complexity. At each of its many levels there are multiple, morphologically distinct subdivisions. Many of these subdivisions contain complete functional representations of the cochlear sensory epithelium. The divergent and convergent patterns of connection between each level of the neuroaxis are elaborate. In order to understand how information is processed within the auditory nervous system it is important to have knowledge of the spatial organizations of these connections.

This study was directed at elaborating the three-dimensional details of the connections to and from several subdivisions at one connectional level—the geniculocortical system. The thalamocortical and corticothalamic projections of the "second" auditory field (AII) and the anterior auditory field (AAF) were studied. The connections of the "primary" auditory field (AI) with the thalamus (Colwell and Merzenich, '80) were used to provide a second referent that, along with the neuronal architecture, enabled a more detailed understanding of the complex connections of AAF and AII with the MGB.

The following specific questions were addressed.

1. What are the *forms* (in three dimensions) of the arrays of neurons from the several subdivisions of the auditory thalamus that project to restricted loci in each of these cortical fields? Likewise, what are the forms of the terminal fields in the subdivisions of the thalamus that arise from the projections of restricted loci in these three cortical fields?

2. What are the *topographic organizations* of the connections of these cortical fields with the subdivisions of the auditory thalamus, and how do they relate to the functional organization of these cortical fields and target nuclei?

3. How are the connections of these three cortical fields with the thalamus *similar* and how are they different?

These questions were addressed by using anterograde (tritiated amino acids) and retrograde (horseradish peroxidase) tracing techniques, which allowed a reconstruction of the three-dimensional structure of the terminations and the sources of the projections. An investigation of the topographic order of the connections of the cortical fields with respect to their internal functional architecture was made possible by deriving limited maps of these fields using microelectrode recording techniques. Thus, the sites of injections of tracers were typified in terms of the internal "cochleotopic" organization for the AAF and AI cortical fields. By systematically varying the positions of tracer injections within these fields according to their "cochleotopic" order, the topographic organizations of the connections of these fields with the thalamus were demonstrated. Additionally, a two-injection paradigm was employed by which the connections of the three auditory fields with the medial geniculate body (MGB) could be directly compared in individual cats.

These studies revealed the complex three-dimensional structure of the interconnections of MGB subdivisions and the three auditory cortical fields, AI, AII, and AAF. AAF connections were very similar to those of the "primary" auditory cortical field, AI. The connections of AII were completely different. These results and those of others (Winer et al., '77; Casseday et al., '76; Rose and Woolsey, '58; Diamond et al., '58; Graybiel, '73) were consistent with a hypothesis that there are two largely segregated auditory projection systems: a *cochleotopic system* providing input to the cochleotopically organized fields (including AI and AAF) via the rostral two-thirds of the MGB and the lateral posterior group, and a *diffuse system,* providing input to noncochleotopic cortical fields (including AII) principally via the caudal aspect of the MGB.

METHODS

Animal preparation, stimulation, and recording

Successful cortical recording-injection experiments were performed in 39 hemispheres of 28 cats. The protocol for animal preparation was similar to that described by Merzenich and colleagues ('75) and Knight ('77). Adult cats were anesthetized with an intramuscular injection of ketamine hydrochloride (25 mg/kg), and 6 mg doses were subsequently administered to maintain a surgical level of anesthesia. A craniotomy was performed over the cortical field or fields of interest and the dura was carefully resected. A photograph was made of the cortical surface and vasculature. A 10 × working print with an overlying .5 mm grid was made and was used to record the sites of vertical microelectrode penetrations and tracer injections. Recordings were made with glass-coated, platinum-iridium microelectrodes with impedances of 2.5 to 3.5 megohms (at 1.0 kHz). Stimuli were delivered via a hollow flexible tube sealed into the contralateral external auditory meatus with low melting point beeswax. The other end of the tube was sealed into a chamber in which an audiometric driver (Telex Model 61470-07, 10 ohms) was sealed. The stimuli were tone pips of .2 seconds duration with trapezoid envelopes (5 msec rise and fall times) and repetition intervals of .8 to 1.0 seconds. The "best frequency" of a unit (or unit cluster) was determined by finding that frequency at which the unit responded at the lowest sound pressure level. This value was determined by viewing unit discharges on the stimulus-synchronized sweep of an oscilloscope and by listening to the amplifier output fed to a loudspeaker. Best-frequency determinations were made at three or more positions within the responsive zone of cortex in each vertical penetration.

Injection of tracers

Injections of anterograde and retrograde tracers were introduced at locations in auditory cortex that had been physiologically typified with a brief map derived with the microelectrode recording techniques outlined above. In the physiological phase of the study, the location of the cortical field to be injected was defined; the approximate boundaries of the field were determined in the region of the injection; and the approximate axis of "isofrequency contours" (see Merzenich et al., '75) was defined. These partial maps generally required 10 to 20 penetrations in each cortical field. They insured that injections were always made well within given field boundaries.

For anterograde tracing, .1 ml of 4,5 ^{3}H-l-leucine (61 C/mM, .5 mC/ml) was desiccated and redissolved in 5 μl of sterile saline. The final label concentration was 10 μC/μl. For retrograde tracing, saturated solutions of horseradish peroxidase (Sigma type VI) were prepared in 5 μl of sterile saline. For injections of both tracers together, the HRP was dissolved in the leucine solution (Colwell, '75; Trojanowski and Jacobson, '75).

Pressure injections were made with 1- or 5-μl Hamilton syringes with 27- or 31-gauge needles. A glass micropipette was often affixed to the tip of the metal needle with sticky wax.

Injections were made in the middle layers of cortex (500–1000 μ depth). They were made manually over several minutes or by attaching the plunger to the hydraulic microdrive and initiating a continuous rate of advancement that completed the injection in 20 or 30 minutes. Injection volumes ranged between .05 and .5 μl, with .15 and .2 μl the most common volumes of injection. After an injection was completed, the micropipette or needle was left in place for 15 to 30 minutes.

In two experiments where long survival times were used for anterograde tracing, the cortex was re-exposed 1 or 3 days prior to sacrifice and the same loci that had received ^{3}H-l-leucine injections were reinjected with HRP. The previous injection sites had been marked with carbon black.

The *effective* spread of tracers at the injection sites was usually difficult to assess on the basis of examination of the injection site alone. However, it was possible to estimate the effective spread for both tracers by defining the limits of the labelling in the target structure. Small injections (e.g., .1 to .2 μl) of either tracer into AI or AAF produced label in pars lateralis that never occupied more than one-fourth to one-third of the nucleus. AI and AAF occupy about the same cortical surface area (Knight, '77; Merzenich, et al., '77). They are each about 6 mm long across their cochleotopic representations and 4 to 5 mm long along their isofrequency axes in the center of the field. Pars lateralis (Vl) contains one representation of the cochlear epithelium which is not grossly dissimilar in proportional dimensions to the cochlear representation in AI or AAF (Aitkin and Webster, '72). Thus, a rough estimate of 1.5 to 2.0 mm as the upper limit of

the diameter of the effective injection site can be made for Vl. (It was, on the average, roughly 1 mm in diameter.) That this is a reasonable estimate of the limit for the spread of tracer at AAF injection sites was further confirmed in several cases in which two injections were made into different cochleotopic representational sites in AAF. This procedure produced two distinct and completely separated bands of label in Vl, even when the injections were placed only 2 mm apart on the cortical surface (see Fig. 11 for a representative example).

Anatomical procedures

Postoperative survival periods were either short (2 days) or long (8 to 18 days). Longer survival times increased autoradiographic labelling of fiber tracts (Cowan et al., '72; Hendrickson, '72) and increased the level of labelling of terminal fields.

Following the postoperative period, animals were anesthetized with sodium pentobarbital and perfused intracardially with cold heparinized saline (4°C) followed by cold .2 M phosphate buffered 2.5% paraformaldehyde solution (pH 7.6). Brains were removed from the skull and placed in cold fixative overnight. The brains were then passed through a graded series (5, 15, 30%) of cold .1 M phosphate buffered (pH 7.6) sucrose solutions over a 24-hour period.

Brains were blocked anterior to the injection sites and posterior to the inferior colliculi and were sectioned serially in the frontal plane on a freezing microtome. Sections were collected on a 90, 30, and 30 μ rotating schedule or on a 100, 50, and 50 μ schedule. The 90 or 100 μ sections were incubated for 10 to 20 minutes in a .07% solution of 3,3'-diaminobenzidine in Trisma buffer (pH 7.6) with hydrogen peroxide (Graham and Karnovsky, '66; LaVail and LaVail, '72; Ralston and Sharpe, '73; LaVail et al., '73) except in two cases in which the tissue was reacted according to Hanker, et al., ('77). One serial set of 30 or 50 μ sections was also processed for HRP and subsequently processed for autoradiography (Colwell, '75; Trojanowski and Jacobson, '75). This combined technique allowed the simultaneous demonstration of HRP and autoradiographic labelling in single sections. The third set of sections was processed for autoradiography alone (Cowan et al., '72). Exposure times for the autoradiograms were generally 3 months.

Data analysis

Sections were examined under bright-field and dark-field illumination with a Zeiss Photomicroscope III or a lower power Olympus Photomicroscope. Low-power dark-field photomicrographs were made of autoradiograms using a Nikon Ultraphot mounted over a Sage (model 281) stereo light box. Photomicrographs were made with Kodak High Contrast Ortho Process 4 × 5 sheet film or with Kodak Panatonic X 35 mm film. HRP-labelled cells were plotted only if the cell bodies or proximal dendrites contained the darkly stained HRP reaction granules seen under high-power bright- or dark-field illumination. This method avoided false identification of labelling in cells with endogenous peroxidase activity (Wong-Riley, '76). HRP-labelled cells were located on dark-field photomicrographs (see Figure 17).

The auditory cortical fields

The approximate positions of the cortical fields on which this study focused (AI, AII, and AAF) are shown in Figure 1. Most of AI in the cat is usually located in the middle ectosylvian cortex (although its location may vary from animal to animal). AI contains a complete representation of the cochlea (Woolsey and Walzl, '42; Hind, '53; Merzenich, et al., '75), with the basal cochlea (high frequencies) represented rostrally and the apical cochlea (low frequencies) represented caudally. Limited sectors of the cochlea are represented along bands that are oriented approximately dorsoventrally within the field (Merzenich et al., '75; Tunturi, '50). The anterior auditory field is located anterior to AI and also contains a complete and highly ordered representation of the cochlea (Knight, '77). AAF shares a high-frequency border with AI; successively lower frequencies within AAF are represented along "isofrequency contours" located successively more anteriorly and ventrally on the anterior ectosylvian gyrus (Knight, '77). AII is located in the general region of the middle ectosylvian gyrus ventral to AI (Woolsey, '60). Unlike AI and AAF neurons, which have relatively sharp tuning curves, AII neurons have relatively broad tuning curves (Hind, '53; Merzenich et al., '75), and it is very difficult to demonstrate any internal representational order within the AII cortical field.

The cortical loci of tracer injections are shown in figure 2 for cases illustrated in this study.

Basis of the parcellation of the medial geniculate body used in this study

It is difficult to determine the boundaries of the subdivisions of the medial geniculate body

(MGB) made on the basis of Golgi techniques in Nissl-stained material (see Fig. 3). In order to define unequivocally the thalamic sources and destinations of the thalamocortical and corticothalamic projections, we paid special attention to the parcellation of the MGB. The morphology of MGB subdivisions was examined using two methods: 1. The Nissl cytoarchitectural structure was revealed in autoradiographic and HRP material counterstained with cresyl violet or neutral red. 2. To obtain a limited view of the dendritic morphology of the neurons, multiple and large injections of HRP were made in the cortex to increase staining of the dendritic processes. Proximal dendrites were visible under the light microscope using this technique.

In the HRP material, we could identify pars lateralis (Vl), pars ovoidea (Vo), and the ventral lateral nucleus (VL) of the ventral division; the deep dorsal nucleus (Dd) and caudal dorsal nucleus (Dc) of the dorsal division; and the medial division (M). The positions of these nuclei and the morphology of the neurons within these nuclei, recorded from this material, concurred with the observations of Ramón y Cajal ('55) and Morest ('64, '65).

Comparison of HRP material with alternate sections of counterstained Nissl material enabled us to compare directly subdivisions made on Nissl cytoarchitectural bases (Rioch, '29; Rose, '49; Moore and Goldberg, '63) with those made on the basis of dendritic morphology (see Fig. 3). The pars principalis includes all subdivisions of the ventral division of MGB, as well as the caudal dorsal nucleus and the dorsolateral aspect of the deep dorsal nucleus. The pars magnocellularis includes the medial division and the ventromedial aspect of Dd. These correlations are in general agreement with those made by Morest ('64).

Once the divisions made on the basis of dendritic morphology were recognized in both the HRP material and the alternate counterstained Nissl sections, it was far easier to identify the various divisions in Nissl-stained material alone on the basis of cell size and packing densities. The packing densities of the various subdivisions were in general agreement with those of Morest ('64), with Vl having the greatest density, followed by the dorsal division, and VL and M being the least densely packed. We would add that pars ovoidea is less densely packed than pars lateralis. Also, in the tracing experiments to be described in the results, HRP injections provided dendritic profiles which assisted in the proper assignment of nuclear origin.

Although we could observe the position of the subdivisions of the MGB made on the basis of dendritic morphology in Nissl-stained sections, it was still not possible to draw the exact borders between some of these subdivisions; there was sometimes .25 mm of uncertainty regarding the location of these borders. For instance, in the top section of Figure 3 it can be seen that the division between the ventral aspects of Dd and Vl is quite clear, with these two nuclei being separated by white matter. However, the absolute border between the rostral aspect of Vl and the caudal aspect of Dc is less clear, as can be seen in the bottom section of Figure 3. Because of the uncertainty as to the exact position of the borders between some nuclei, we have not drawn borders around subdivisions on the sections shown in the following figures since these borders would be in some cases only approximate and thus artificial.

RESULTS

AI connectivity with auditory thalamus

It is appropriate to describe thalamocortical and corticothalamic projection arrays defined with small injections in AAF and AII in relation to: a) the cytoarchitectural subdivisions of the MGB, and b) the projection arrays defined with small injections into functionally corresponding loci in AI. Therefore, it is necessary to describe the basic features of the corticothalamic and thalamocortical arrays projecting from and to restricted AI loci. This AI-MGB connectional data confirms and extends the descriptions of AI connections defined in similar studies using the same techniques (Colwell and Merzenich, '80).

The corticothalamic and thalamocortical projections of AI were investigated by placing single (or occasionally multiple) microinjections of ^{3}H-l-leucine or HRP at physiologically defined loci within the field. Successful experiments were performed in the AI auditory fields of 19 hemispheres. The physiologically typified loci of injections had best frequencies ranging (in different experiments) from 1.5 to 25 KHz. As Colwell and Merzenich ('80) have shown, corticothalamic and thalamocortical AI projection arrays are virtually identical; i.e., there is a remarkably faithful reciprocal interconnection of discrete cortical loci with complex thalamic arrays. Given this remarkable reciprocity, a description of the corticothalamic projection arrays from restricted AI loci constitutes an accurate description of the

figures of the thalamic cell arrays projecting to those same cortical loci.

Corticothalamic projection of AI

After AI injections of ^{3}H-l-leucine and short survival times (2 days), fibers were followed from the cortical injection site to the thalamus (see Fig. 4). Fibers left the injection site as a tight bundle arching ventrolaterally. Corticothalamic fibers descended from this bundle in a broader, anastomosing group in the internal capsule. The remaining fibers continued medially in the frontal plane, arched dorsally, and entered the corpus callosum (destined for contralateral auditory cortical areas). The corticothalamic tract coursed ventral and lateral to the rostral pole of the lateral geniculate nucleus. Fibers entered the reticular nucleus of the thalamus lateral to the lateral posterior group of the dorsal thalamus. Dense pericellular clustering of autoradiographic grains around cells in the reticular nucleus indicated terminal fields in this region (see Fig. 4).

Corticothalamic fibers continued medially through the reticular nucleus ventral to the LGN and entered the lateral division of the posterior group of the thalamus. Labelling within the POl was complex: at least two and often as many as four or five foci of autoradiographic (ARG) labelling were commonly seen after single restricted AI injections.

Caudal to the posterior group, two descending profiles (one medial and one lateral) of continuous ARG labelling coursed caudalward from the rostral pole of the MGB. The medial column of ARG label was continuous rostrally with the label in POl. This columnar figure passed along the rostrocaudal axis for about 2 mm from the rostral pole of the MGB into the rostral aspect of the caudal third of the geniculate before attenuating (see Fig. 5). Examination of these sections counterstained with Nissl stains and examination of the morphology of the HRP-containing neurons of this cell array after injections of HRP into AI revealed that this column extended through the deep part of the dorsal nucleus rostrally and extended into the medial nucleus of the MGB caudally (Figs. 5, 12, and 13).

The lateral ARG-defined corticothalamic projection was sheetlike in form. It began at the rostral pole of the MGB and ended caudally in the rostral aspect of the posterior third of the MGB, at about the same level as the end of the labelled medial column. The lateral array first appeared rostrally, in the transverse plane, as a band along the dorsolateral margin of the MGB, parallel to its surface. This grain field was situated in the rostral aspect of the pars lateralis of the ventral division (see Fig. 13, sec. 15). As the sheetlike projection extended caudally in pars lateralis, it moved inward from the surface of the MGB and acquired a more vertical orientation (see Fig. 5, sec. 10; Fig. 16, sec. 17).

In the middle third of the MGB, the sheetlike projection divided to form, in frontal sections, a larger sheet of label in pars lateralis and a smaller sheet or column of label in pars ovoidea (see Fig. 6). Caudal to the level at which this label in Vo first appeared in frontal sections, the ARG-labelled terminal fields in Vl and Vo were continuous, and together formed an inwardly folded terminal field array (see Fig. 5, sec. 16). Thus, three dimensionally, Vl and Vo form a continuous sheet about 2

Abbreviations

AAF	anterior auditory field
AES	anterior ectosylvian sulcus
AI	first auditory field
AII	second auditory field
ARG	autoradiography
BIC	brachium of the inferior colliculus
CP	cerebral peduncle
D	dorsal division of MGB
Dc	caudal dorsal nucleus of the MGB
Dd	deep dorsal nucleus of the MGB
Ds	superficial dorsal nucleus of the MGB
EE	ipsilateral and contralateral ear stimulation, both excitatory
EI	ipsilateral ear excites, contralateral inhibits
Ep	posterior ectosylvian auditory field
HRP	horseradish peroxidase
IC	inferior colliculus
ICC	central nucleus of the IC
ICP	pericentral nucleus of IC
ICX	external nucleus of the IC
I-T	insular-temporal cortical region
LGN	lateral geniculate nucleus
M	medial division of the MGB
MGB	medial geniculate body
MGm	pars magnocellularis or magnocellular division of the MGB
MGp	pars principalis or principal division of the MGB
OT	optic tract
PAF	posterior auditory field
PES	posterior ectosylvian sulcus
PO	posterior group of thalamus
POl	lateral division of PO
R	reticular nucleus of the thalamus
SS	suprasylvian sulcus
T	temporal cortical region
TAA	tritiated amino acids
Vl	pars lateralis of the ventral division of the MGB
VL	ventral lateral nucleus of the ventral division of the MGB
Vo	pars ovoidea of the ventral division of the MGB
VPAF	ventral posterior auditory field
Vt	transitional zone of the ventral division of the MGB

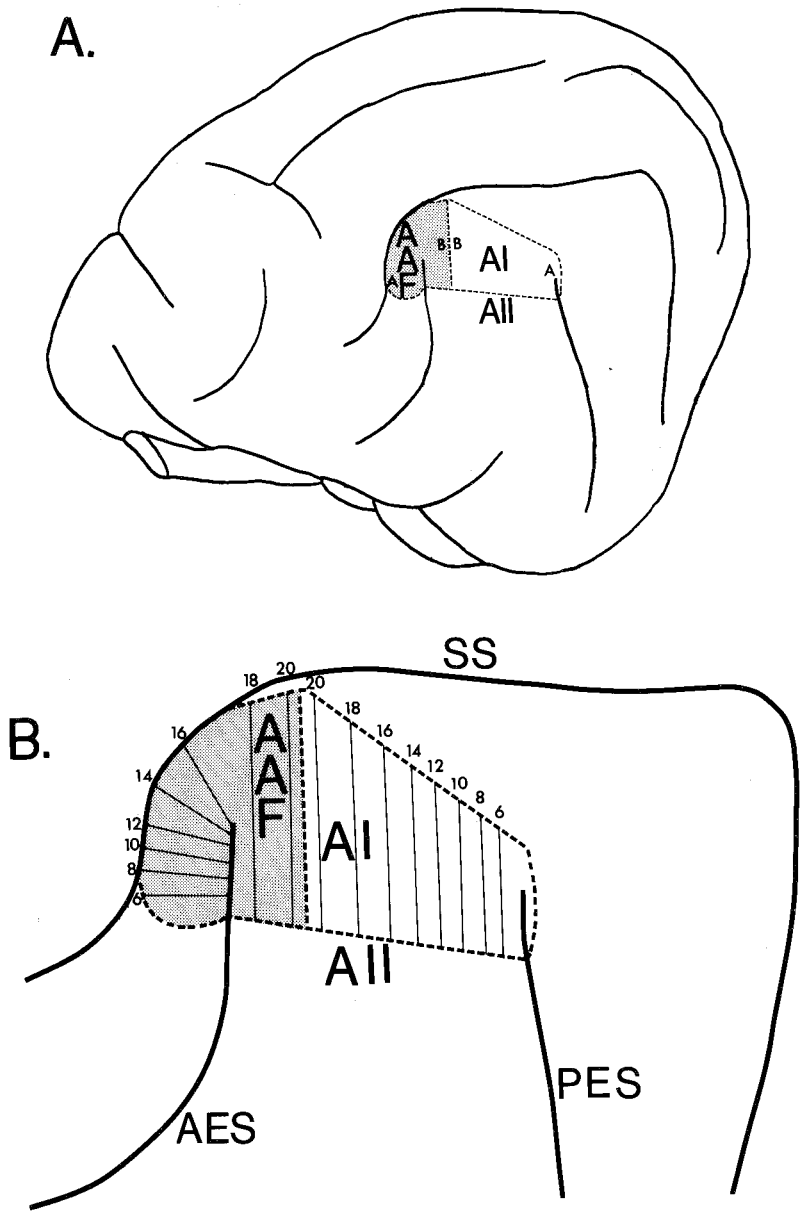

Fig. 1. A is a surface view of the left lateral side of a cat brain. In this figure, the relative positions of the three cortical fields examined in this study are represented with respect to the sulcal patterns (the position of these cortical fields with respect to the sulci are not to be taken literally but only as an average or typical example; see Merzenich, et al., '75). The subscripts A and B indicate apical (A) and basal (B) positions in the cochlear representations within AI and AAF. In B, the isofrequency contours are indicated along the lines within AAF and AI. In this figure, the frequencies have been converted to cochlear place in millimeters from the apex. SS: suprasylvian sulcus; AES: anterior ectosylvian sulcus; PES: posterior ectosylvian sulcus. This figure is modified from Merzenich et al. ('77).

INJECTION SITE CENTERS

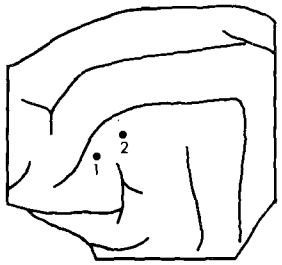

76-133 LEFT
1) AAF: TAA & HRP, 1.5 KHZ
2) AAF: TAA & HRP, 25 KHZ

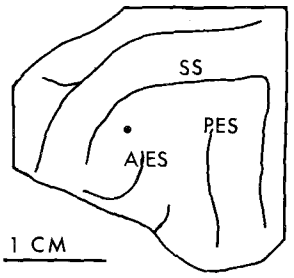

76-133 RIGHT
AAF: TAA & HRP, 2.5 KHZ

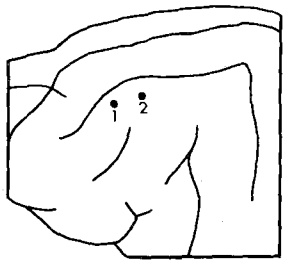

77-14 LEFT
1) AAF: TAA & HRP, 2 KHZ
2) AAF: TAA & HRP, 14 KHZ

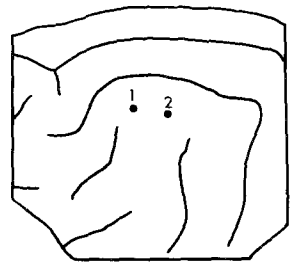

77-14 RIGHT
1) AAF: HRP, 13 KHZ
2) AI: TAA, 13 KHZ

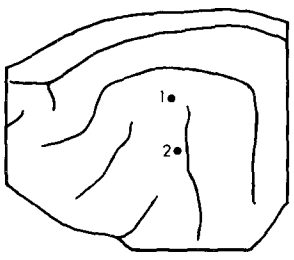

77-1 LEFT
1) AI: TAA, 6 KHZ
2) AII: HRP

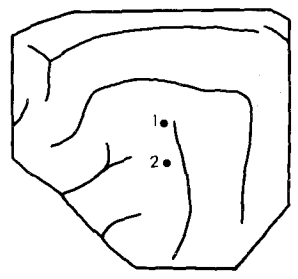

77-1 RIGHT
1) AI: TAA, 3 KHZ
2) AII: HRP

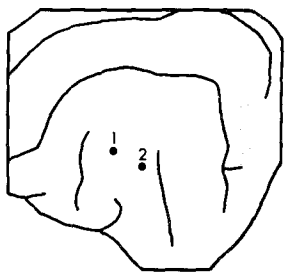

76-140 RIGHT
1) & 2) AII: HRP & TAA

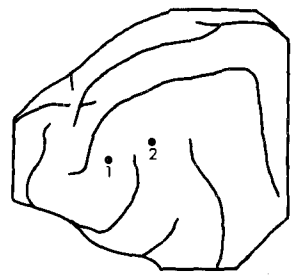

77-12 LEFT
1) AAF: HRP, 11 KHZ
2) AI: TAA, 11 KHZ

Figure 2

mm long in the rostrocaudal dimension. In the rostral aspect of the MGB the sheet passes through Vl only, and caudally it passes through Vl and Vo. In the middle aspect of the MGB, the division of Vl into Vo and Vl produced a hole in this otherwise continuous sheet.

A focus of ARG label appeared rostrally, just preceding the most rostral appearance of Vo, in the medial aspect of the ventral division (see Fig. 5, sec. 13; Fig. 16, sec. 17). This label became the medial point of folding for the infolded sheet caudally (see Fig. 5, sec. 13 and 16); i.e., it constituted the most medial sector of this folded sheet. Caudally, this region had larger cells than those of Vl. These neurons were, in fact, similar to the cells of Vo. This focus of ARG label was thus believed to be in the dorsal part of pars ovoidea. It appeared to correspond to the "transitional zone" of Morest ('65), and hence was labelled Vt in Figure 5 and in subsequent illustrations. There was always a region of lighter label between the Vt and Vo components of the folded sheet (Fig. 5, sec. 16).

Topographic organization of the AI projection onto the MGB

Injections at different physiologically determined locations in AI revealed that all nuclei of the MGB which received projections from (and project to) AI were topographically interconnected with it. The systematic topography noted in these experiments was the same as the topography described by Colwell and Merzenich ('80).

With injections of anterograde tracer into the sites of representation of successively higher frequencies within AI, the sheetlike labelled arrays in the ventral division shifted medially, dorsally, and rostrally, and the columnar arrays of label in Dd-M shifted more dorsally, laterally, and rostrally.

Discontinuities in the AI projection

Almost invariably, injections into the higher frequency part of AI resulted in four or five patches of relatively intense ARG label within the caudal infolded sheet of label in the ventral division (Fig. 5, Sec. 16). Between the intensely labelled regions, ARG grain density dropped to relatively low levels. There appeared to be an increased likelihood of distinctive periodic discontinuities of labelling if small injection volumes (i.e., 1 μl) were used.

Three-dimensional reconstructions revealed that the patches of label were parallel columns or bands, with their long axes oriented rostrocaudally in the nucleus (see Fig. 7). When this banding was seen, two or three bands were in Vl, one was in Vt, and one was in Vo.

Combined HRP-leucine injections into high-frequency regions of AI also produced banding of HRP-labelled cells in the caudal aspect of the ventral division. These HRP-labelled cell bands were identical in form and coincident with the autoradiographically labelled bands.

With injections at low-frequency representational sites in AI, a distinct banding pattern was not seen in pars lateralis, although a suggestion of a periodic pattern was seen in two cases.

Connections of AAF with the thalamus

There were 17 successful cases in which microinjections of HRP were placed in AAF and 13 successful cases in which ^{3}H-l-leucine microinjections were made into AAF. The physiologically typified loci of injections spanned five octaves (1.5 to 25 kHz) and were evenly distributed over this range.

The thalamocortical connections of AAF

Single injections of HRP into AAF produced multiple groups of labelled neurons in POl (see Fig. 8, sec. 27). Caudal to the posterior group, two components of labelled neurons, one located medially and one laterally, extended through the rostral and middle thirds of the MGB. The medial component was virtually identical in form to that seen with functionally corresponding AI injections, although neurons were often more intensely labelled than with equal volume injections into AI. The medial component was rostrally continuous with the HRP-labelled cells in POl. The label extended as a column, in the rostrocaudal dimension, for about 1.5–2.0 mm through the deep dorsal nucleus, to end in the medial division (Fig. 8; Fig. 9; Fig. 11, sec. 20;

Fig. 2. Representations of the cortical loci of tracer injections for the cases illustrated in the following figures. The line drawings of the sulcal patterns were made from photographs of the post morten cat brains. The injection sites were located from photographs of the surgically exposed brains made during the recording phases of the experiments (see methods) and by locating carbon black marks made at the injection sites. Both right and left sides of the brain have been oriented so that rostral is to the reader's left and caudal is to the reader's right. Since the photographs from which the drawings were made did not include the entire brain, the straight edges of the drawings indicate the limits of the photographs.

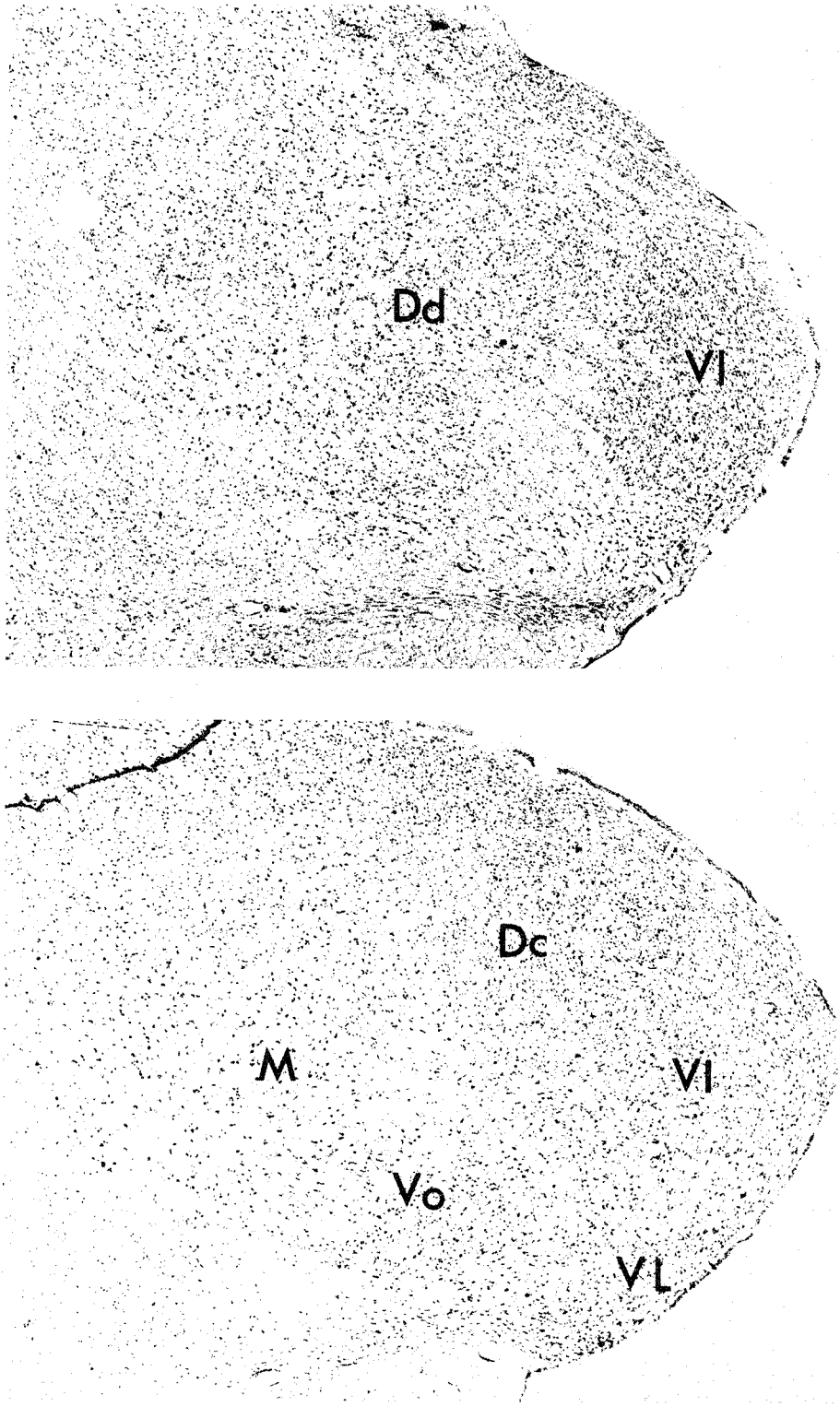

Fig. 3. Nissl-stained frontal sections through the MGB. The sections in all the figures are in the transverse (frontal) plane. The top section is taken through the rostral third of the MGB and the bottom section through the middle third. Dd: deep dorsal nucleus; Vl: pars lateralis; Vo: pars ovoidea; M: medial division; Dc: caudal dorsal nucleus; VL: ventral lateral nucleus.

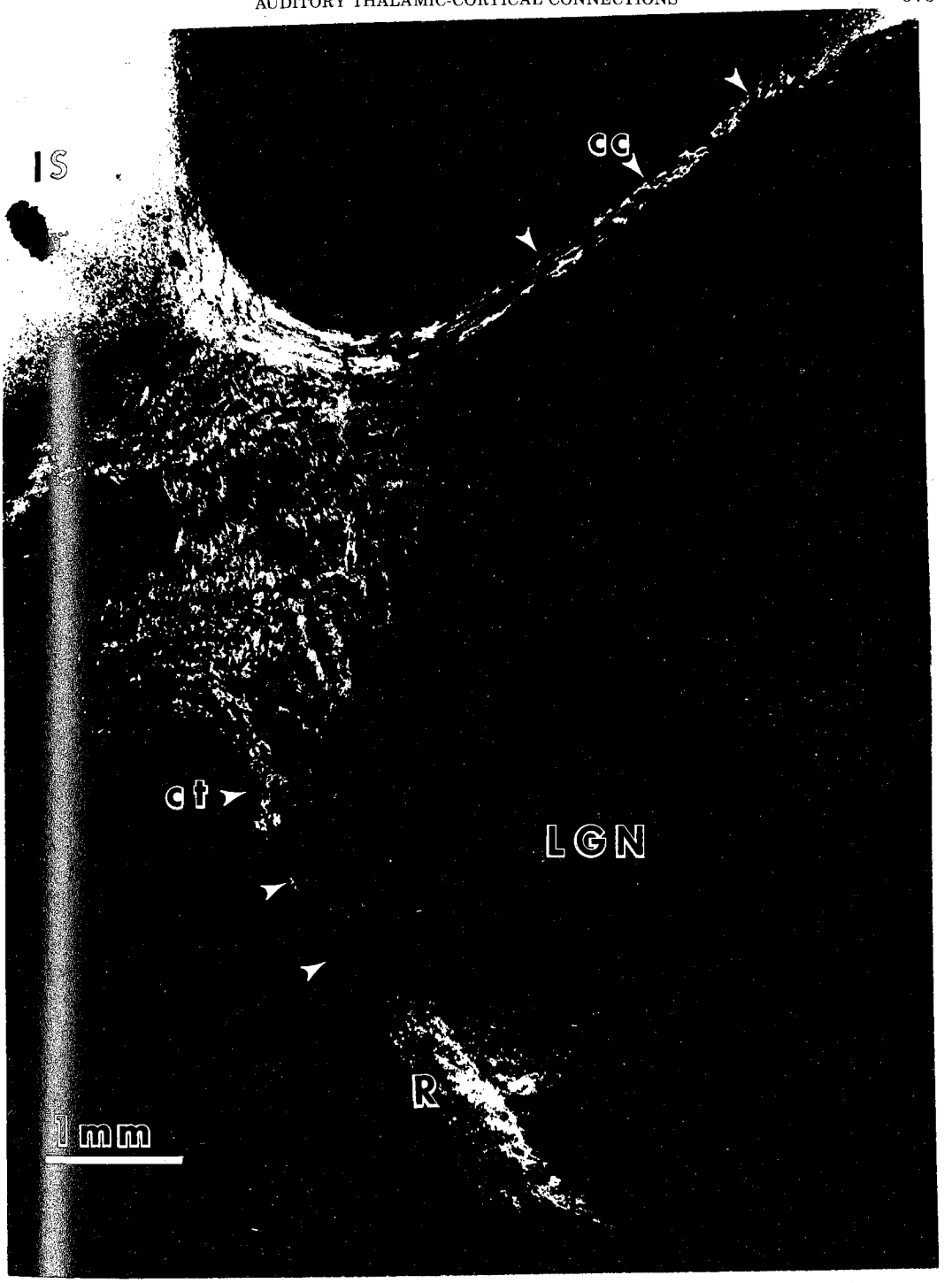

Fig. 4. An example of the path of cortical efferent fibers leaving a ^{3}H-l-leucine injection site in AI. The injection site is the bright white area in the upper left hand corner labelled IS. The transcallosal corticocortical fibers (CC) arch dorsomedially from the injection site and, in the upper right hand corner of the dark-field photomicrograph, these fibers enter the corpus callosum. The labelled corticothalamic fibers (which are probably intermingled with labelled corticotectal, corticopontine, and corticostriatal fibers) course ventrally in a broader, anastomosing pattern (CT). The course of the labelled fibers, portions of which dropped out in this reproduction but which were visible under the microscope, is indicated by the white arrows. Heavy ARG terminal labelling from this projection is present in the reticular nucleus of the thalamus (R), ventrolateral to the lateral geniculate nucleus (LGN).

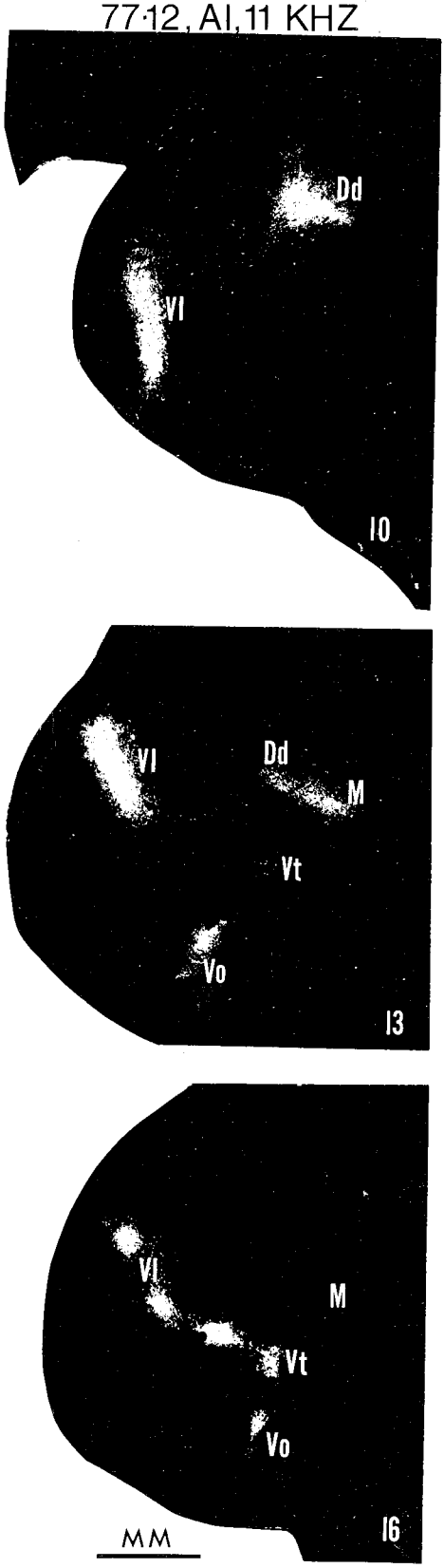

Fig. 13, sec. 23). Labelled cells in the medial division were scattered more than in Dd; in other words, the packing density was much less for M than Dd. Cells labelled in Dd after AAF injections were stellate and were of medium size, whereas in M, HRP-labelled cells were large and multipolar. The intensity of HRP labelling within individual cells in M was consistently not as great as in Dd.

The lateral component of labelled neurons also appeared to be in the same region as the AI thalamocortical projection arrays. However, HRP labelling in the ventral division after AAF injections was always more discontinuous than that seen after homotypic AI injections. With AAF injections, cells in the ventral division were almost invariably clumped and occupied only limited sectors of the sheets through Vl, Vt, and Vo defined by the AI projection arrays (Fig. 8, sec. 43 and 45; Fig. 9, sec. 69; Fig. 11, sec. 18). Occasionally, a single clump of cells was labelled in the rostral Vl and appeared roughly as a column oriented rostrocaudally. More often, a single intensely labelled clump or column was present, but a few scattered neurons were also seen in other regions of Vl. When this situation occurred, the overall distribution of cells, at least in the rostral Vl, approximated a broken sheet oriented rostrocaudally (Fig. 11, sec. 18). Quite often, the column of high-density labelling in the rostral half of Vl appeared along its ventral aspect (Fig. 11, sec. 18). Overall, the

Fig. 5. Representative example of the corticothalamic projection of AI onto the MGB. A .1 μl (2μ C) ^{3}H-l-leucine injection was made at an 11 kHz locus in AI (See Figure 13 for the microelectrode map of the cortical surface and the position of the injection site.) Each section number represents a sequential 200 μ step. The dark-field photomicrograph of Section 10 is taken from the anterior portion of the rostral third of the MGB; section 13 from the posterior portion of the rostral third of the nucleus; section 16 from the anterior portion of the middle third of the MGB. The nucleus is 3.6 mm in the rostrocaudal dimension of this cat, beginning with section 9 rostrally and ending with section 27 caudally. There is no labelling after section 19; in all cases after AI injections the posterior third of the MGB was unlabelled.

The projection comprises, laterally, a continuous sheet of labelled terminals in the ventral division which is rostrally in the form of a lamina in Vl (section 10) and caudally is in the form of a folded sheet (section 16) which includes Vl, Vo, and the "transitional zone" (Vt) (note that there are often periodic discontinuities in the intensity of labelling in the caudal aspect of the sheet projection—section 16). Medially the projection is in the form of a continuous column of label, which passes through Dd rostrally (section 10) into M caudally (sections 13 and 16). The lateral sheet and medial column of labelled terminals are both about 2 mm long in the rostrocaudal dimension in this case.

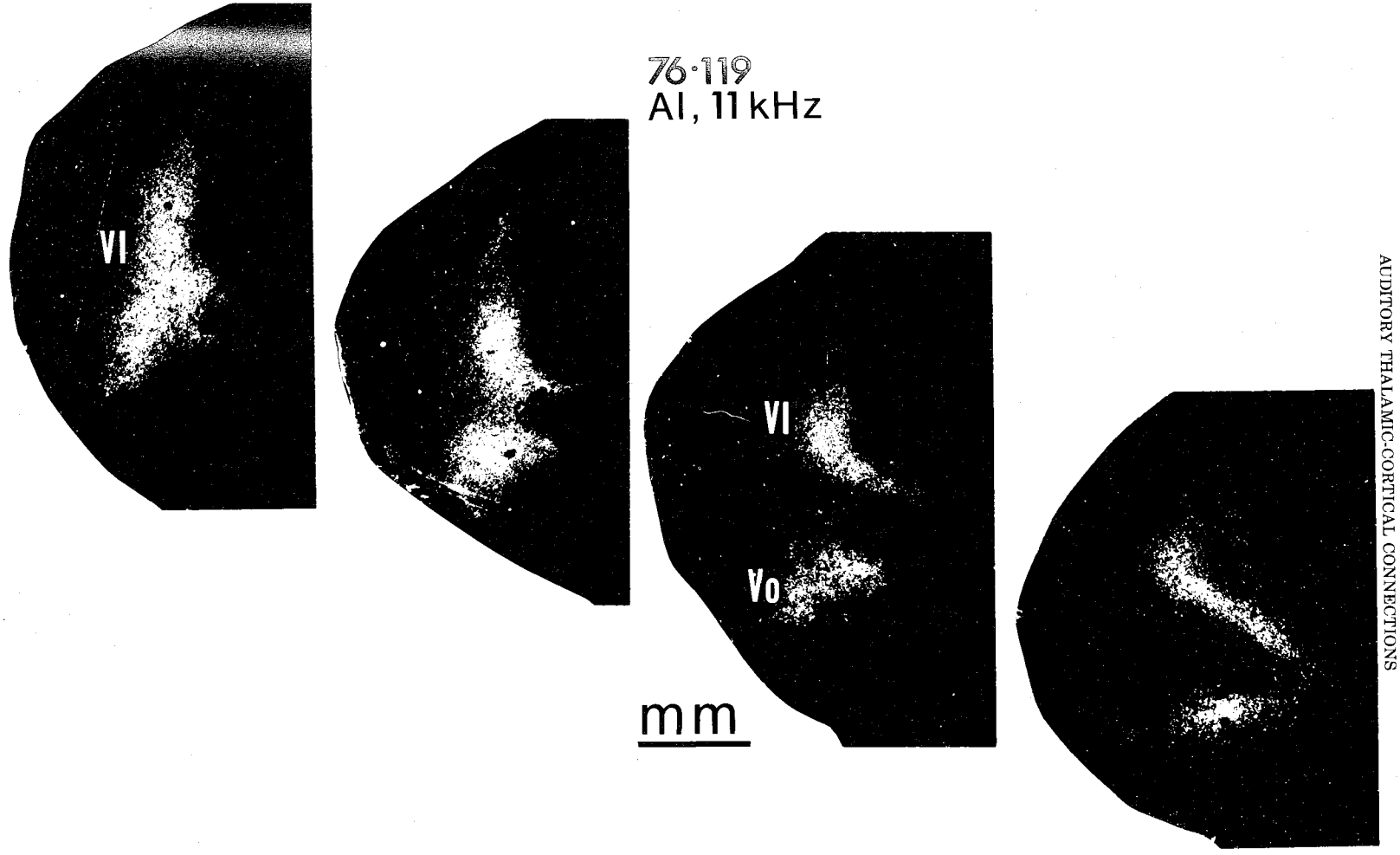

Fig. 6. Two representative examples of how pars ovoidea of the ventral division is derived from a split in pars lateralis of the ventral division. The sequential sections represent 150 μ steps. Sections from more rostral levels are placed on the left and sections from more caudal levels are located to the reader's right.

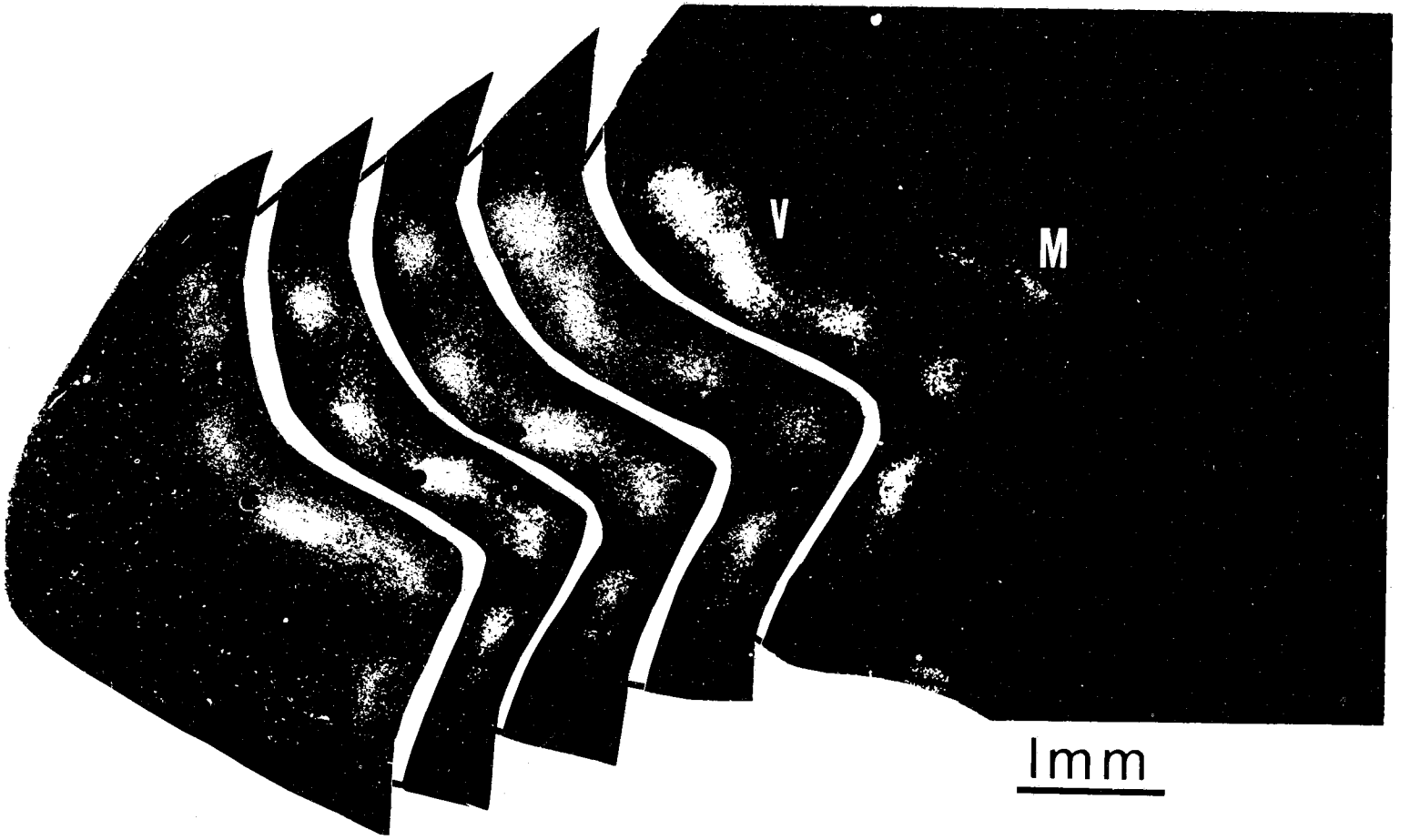

Fig. 7. An example of banding in Vl of the corticothalamic projection. Adjacent sections (taken from the same case represented in Fig. 5) have been aligned with the most caudal on the left and the most rostral on the right. The discontinuities of label in Vl (the top three groups of patches), Vt (the most medial patches), and Vo (the bottom patches), in three dimensions, are in the form of parallel columns oriented rostrocaudally. This banding is restricted to the caudal half of Vl, just caudal to the partition of Vl into Vl and Vo. This banding was noted only after small volume injections at higher frequency representational loci in AI (and AAF).

number of cells labelled in the ventral division after AAF injections of HRP was far lower than the number which resulted from equal-volume AI injections. As with AI injections, labelled cells in Vl were of medium size and in general had ovoidal or fusiform cell bodies. In the frontal plane, the cells had proximal dendrites that tended to be aligned along the long dimensions of the sheets defined by the AI and AAF projection arrays.

Corticothalamic projections of AAF

The corticogeniculate fiber path of AAF into the thalamus was similar to that taken by AI corticothalamic fibers. In only one case was autoradiographic label seen in the reticular nucleus of the thalamus; however, this labelling was located much further rostrally than after AI injections. Since this was also the only case in which the thalamus was sectioned that far rostrally, it is probable that the autoradiographic label in the reticular nucleus was missed in other experiments.

Single injections of ^{3}H-l-leucine in AAF resulted in corticothalamic projection arrays that were similar in form to those seen with AI injections (see Figs. 8, 9, 10, and 11). Unlike the AI corticothalamic arrays, the label in Dd was relatively more intense, and the label in the ventral division was relatively less intense (see Figs. 8, 9, 10, and 11). In fact, the ARG labelling in the ventral division, although always present, was often so light as not to appear in the dark-field photomicrographs (see Figs. 8 and 9).

Reciprocal relationship of the thalamocortical and corticothalamic connections of AAF

In 11 of these cases, mixtures of both ^{3}H-l-leucine and HRP were injected at single physiologically defined loci in AAF. These combined injections always produced spatially related (and partially superimposed) patterns of label in POl and MGB. Results from sections processed for both tracers showed that all HRP-labelled cells were overlain by the restricted autoradiographic arrays. The autoradiographic label pattern was highly reciprocal with the medial cell column (POl, Dd, M; see Figs. 8 and 9) and was relatively continuous over the always patchy and often strikingly discontinuous lateral thalamocortical cell array (Vl, Vo, Vt; see Fig. 11).

Topographic organization of the AAF projection to and from the MGB

The systematic topography of the thalamocortical and corticothalamic connections of AAF and AI are alike in every respect (with the exception that the connections of AAF with the ventral division are relatively weaker). Thus, tracer injections at successively higher frequency representational loci in AAF produced labelled Dd-M columns that were located relatively more dorsolaterally and rostrally (see Fig. 10) and labelled ventral division sheets that were located more dorsomedially and rostrally (see Fig. 11). There was an apparent reversal in the topographic interconnections of AAF along the Dd-Vl border, with the caudal margin in AAF (representing highest frequencies) interconnected along this boundary. There was also an apparent topographic reversal of the representation of the lowest frequencies along the mutual border of Vo and Vl. Away from the Vo-Vl border, successively higher frequency representational sites were connected to successively more medial locations within Vo and in successively more dorsal and medial locations in Vl. A high-frequency reversal at the Vl-Dd border and a low-frequency reversal at the Vl-Vo border were also recorded with AI injections.

Although the Dd-M connections with AAF were systematically ordered with respect to the cochleotopic organization of AAF, the organization was not as precise as were the connections with the ventral division. This imprecision was apparent in comparisons of the regions of autoradiographic labelling of Dd with labelled Vl regions. Examples are illustrated in Figures 10 and 11. In the experiment represented in Figure 11, injections placed at 2 and 14 kHz did not produce two separable ARG-labelled regions in Dd; by contrast, separable labelled regions in Vl were very distinct. In the experiment represented in Fig. 10, injections were placed further apart in the tonotopic map in AAF (1.5 and 25 kHz locations). In this double-injection case, two clearly separable columns of label were evident in Dd. The topography of the Dd-M connections was also noted to be less precise than the ventral division connections for AI.

There was a disproportionately larger representation of higher best-frequency AAF sites in pars ovoidea. With injections within AAF at best-frequency locations of less than about 2 kHz, the sheet of label passing through Vo becomes very thin when compared with labelling resulting from equal volume injections at higher best-frequency locations (e.g., compare Vo_1 in section 20 with Vo_2 in section 23 of Figure 11). A similar disproportionate representation in Vo was recorded for the connections of AI.

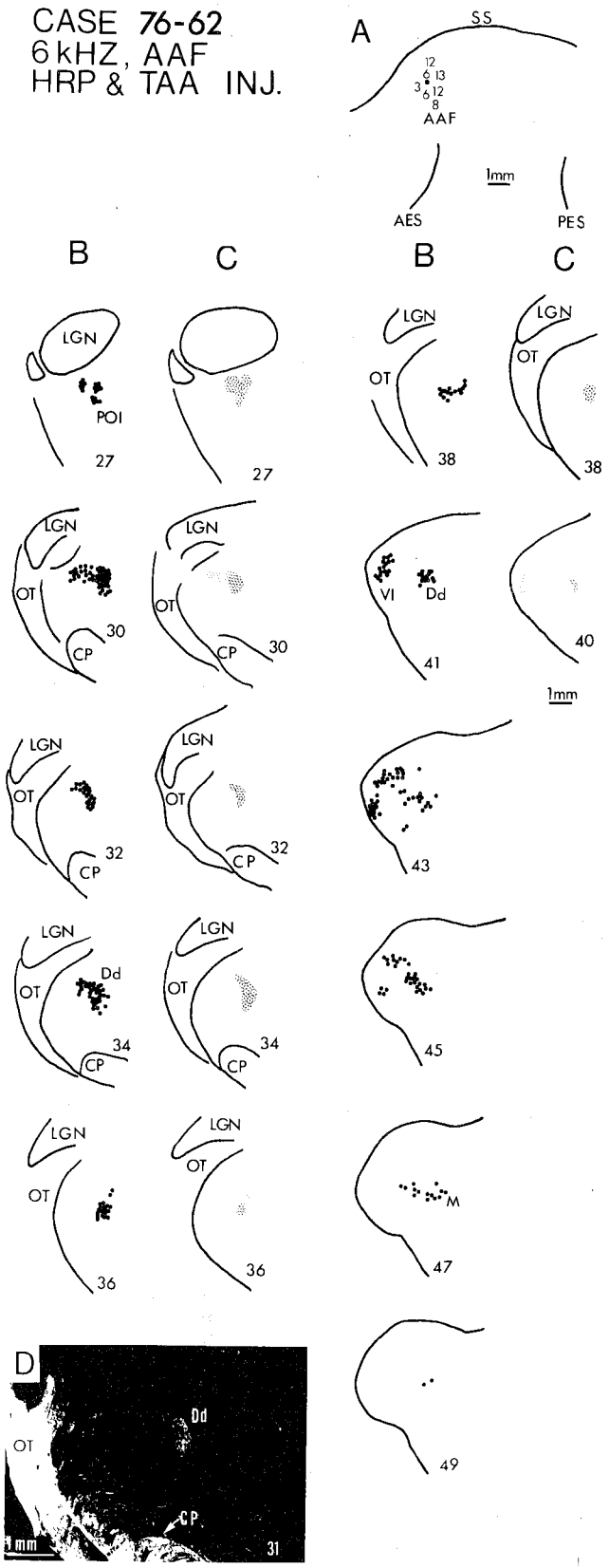
CASE 76-62
6 kHZ, AAF
HRP & TAA INJ.
A
SS
12
13
3
6
12
8
AAF
1mm
AES
PES
B
C
B
C
LGN
POI
27
27
LGN
OT
38
LGN
OT
38
LGN
OT
30
CP
LGN
OT
CP
30
VI
Dd
41
40
1mm
LGN
OT
32
CP
LGN
OT
CP
32
43
LGN
OT
Dd
34
CP
LGN
OT
CP
34
45
LGN
OT
36
LGN
OT
36
M
47
49
D
Dd
OT
CP
1 mm
31

Figure 8

With high best-frequency place injections in AAF (see Fig. 11) or AI (see Fig. 13, sec. 15), the autoradiographic labelling in Dd and Vl often joined at their dorsal borders in the rostral third of the MGB. This apposition of labelled regions apparently reflects the topographic reversal between Dd and Vl that occurs in the projections from the high-frequency representations in AAF and AI.

Banded periodicities in the AAF to ventral division corticothalamic projection

When injections were made at higher best frequency loci in AAF, a banding pattern in the folded sheet of autoradiographic label in the caudal region of the ventral division was often seen. The four or five foci of more dense label (one in Vo, usually one in Vt, and two or three in Vl) appeared to correspond with those seen in AI injection cases (Fig. 11, sec. 23). Perhaps at least partially due to the sparse distribution of HRP-labelled neurons seen with AAF injections, a banded pattern of light and heavy HRP labelling corresponding to the banded pattern seen with the corticothalamic projection array was never clearly evident.

Direct comparison of the AI and AAF connections

Four experiments were performed to obtain a *direct* comparison of the connectional structure and organization of AI and AAF. In these experiments, partial maps of both fields in single hemispheres were made, and single injections of anterograde tracer in AI and retrograde tracer in AAF were made at cochleotopically homotypic locations. Since the connections of AAF and AI with the dorsal thalamus are reciprocal, this protocol directly compares the topographies of the thalamocortical and corticothalamic connections of the two cortical fields in single MGB's. (Although, after combined tracer injections in AAF, the light autoradiographic label in the ventral division was always relatively more continuous than the HRP labelling, the boundaries for the extent of the HRP labelling were always defined by the autoradiographically labelled terminal arrays.)

The results of experiments in which alternate sections were processed for one label and then the other showed that the overall pattern of connections for the two fields was very similar (Fig. 12). In cases where each section was processed for both tracers, HRP-labelled neurons were found only in regions that were overlain with above background ARG label (see Fig. 13). These experiments demonstrated that the thalamocortical and corticothalamic connections of Dd and M with AI and AAF were of the same form and topographic order. The corticothalamic connections of AI and AAF with the ventral division were also apparently topographically identical, with the single exception that the AI projection was much more dense. The thalamocortical projections to AI and AAF from the ventral division were similar in that they were derived from the same regions of the nucleus as defined by the corticothalamic projection of AI. However, within this region, the neurons of the AAF thalamocortical projection array were much more sparse and discontinuously distributed than were the arrays of AI projecting neurons.

AII electrophysiology

AII is located ventral to AI. The border of AI with AII was marked electrophysiologically by an abrupt transition from sharply tuned neurons and a cochleotopic organization within AI to relatively much more broadly tuned neurons and an apparent lack of a cochleotopic organization within AII. Typical AII neurons were almost equally as senstitive (within 10–15 dB) across a broad range of frequencies, commonly spanning several octaves. The AI-AII border was generally oriented ventroposteriorly and dorsoanteriorly. Very extensive maps of AII were made in two hemispheres, in an attempt to define all of its borders. Posteriorly, in the region of the posterior ectosylvian sulcus, AII is bordered by cochleotopically organized regions of cortex (the "posterior auditory field" and the "ventroposterior auditory field"). The broad-tuning region below AI extends for at least 6 mm ventrally. However, on the basis of other differences in recording, it was concluded that this large

Fig. 8. A representative example of the thalamocortical and corticothalamic connections to and from a cortical locus in AAF. In this particular experiment, (76-62), a .5 μl mixture of HRP and ^{3}H-1-leucine (5 μC) was injected at a 6 kHz, best-frequency locus in AAF. A) is a surface view of the cortex. Numbers indicate the best-frequency determination of vertical microelectrode penetrations. The locus of the injection is indicated by the dark spot. B) indicates the HRP labelling, each dot representing a single HRP-granule-containing neuron. Sections are numbered rostrally to caudally in 120 μ steps. C) shows adjacent autoradiograms to the sections in B.

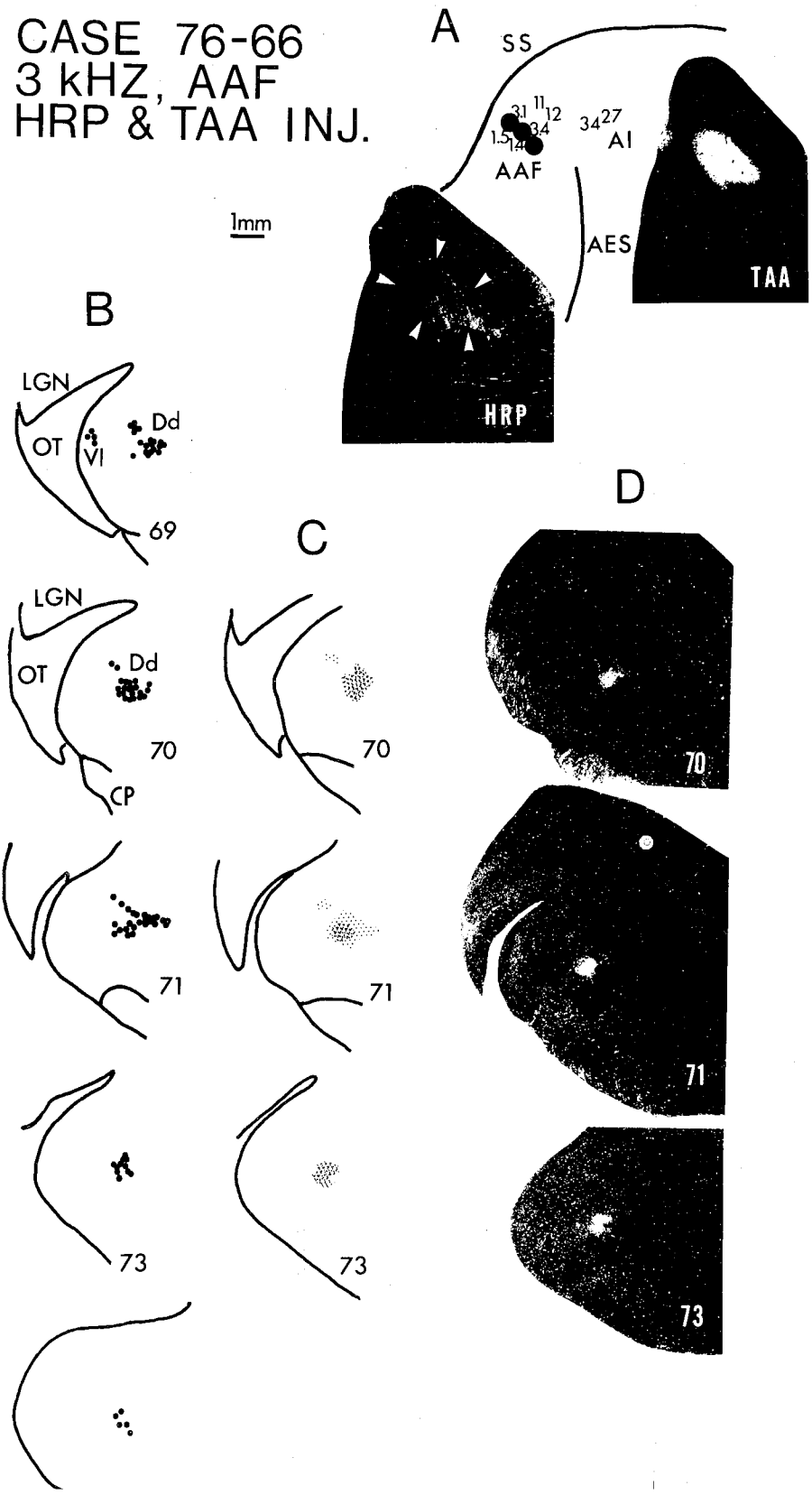
CASE 76-66
3 kHZ, AAF
HRP & TAA INJ.
A
SS
31
11
12
1.5
14
34
34
27
AI
AAF
AES
TAA
HRP
1mm
B
LGN
OT
VI
Dd
69
C
D
LGN
OT
Dd
70
CP
70
70
71
71
71
73
73
73

"AII" region probably contains more than one cortical field with neurons of broad-tuning characteristics. For instance, there was generally a strip of AII that borders AI ventrally, roughly 1 mm in width, in which neurons were more responsive to auditory stimuli. Neurons in this region had lower thresholds, and a greater number of spikes were evoked by equivalent suprathreshold stimuli. Injections were centered within this strip and below it. No obvious difference in the thalamocortical connectivity of this AI-bordering strip as compared with that of more ventral AII cortex was observed.

Because of the uncertainty of the homogeneity of the broad-tuning region ventral to AI, all injections of tracer that are reported in this study were made within a zone about 1 to 2.5 mm ventral to the AI-AII border. Partial maps of the cochlear representation of AI near the AII border were always made prior to injections. This mapping enabled the AII injection sites to be referenced to best-frequency locations along the border of the adjacent AI field.

Thalamocortical connections of AII

In 14 cases, HRP microinjections were placed at physiologically identified loci in AII. These experiments demonstrated that AII receives projections from the caudal and middle thirds of the MGB. The projecting nuclei were the caudal dorsal nucleus (Dc) of the dorsal division, the ventral lateral nucleus (VL) of the ventral division, and the medial division (M). The Dc projection was the heaviest of the three projections in terms of the numbers and packing densities of the labelled cells (see Fig. 17). The VL projection was the next heaviest, followed by M (see Fig. 14, sec. 50).

After injections of HRP into AII, a continuous array of labelled cells could be followed caudorostrally. The caudal pole of the MGB was extensively labelled (Fig. 14, sec. 46 and 48; Fig. 15, sec. 7; Fig. 16, sec. 23, 24, and 26). These neurons were located in Dc. They were medium-sized stellate neurons, and they were commonly closely packed within the projection array. The projection pattern from Dc was complex, with labelled cells often occurring in prominent groups (Fig. 14, sec. 48).

More rostrally, at about the level of the junction of the posterior and middle thirds of the MGB, a label-free region appeared in the lateral aspect of the MGB (Fig. 14, sec. 50; Fig. 15, sec. 10; Fig. 16, sec. 20, 21, and 22; Fig. 17). This label-free region was comprised of the pars lateralis and pars ovoidea of the ventral division. The label-free region was surrounded by a broad band of labelled cells in Dc, VL, and M. The cells in VL were of medium size; the cells in M were large and multipolar. This broad "C" (or reverse "C")-shaped band generally continued rostrally for several hundred microns into the middle third of the MGB.

Corticothalamic fiber projections of AII

In 10 experiments, single microinjections of ^{3}H-l-leucine were placed in physiologically typified AII regions of auditory cortex. From the injection site, corticothalamic fibers were followed into the thalamus. Although labelled fibers passed through the reticular nucleus in a course similar to that of AI and AAF fibers, there was no unequivocal preterminal labelling in the reticular nucleus.

In the rostral third of the MGB, in short survival cases, very light label was sometimes noted along the lateral aspect of the MGB. In the long survival case, this label was more apparent and occurred in fascicles in regions that were free of cell bodies. The tissue in these fascicular regions also transmitted more

Fig. 9. A representative example of the thalamocortical and corticothalamic connections of an isofrequency contour in AAF with the MGB. In this experiment (76-66), three injections (.5 μl each) of a mixture of ^{3}H-l-leucine (5 μC) and HRP were made along a 3 kHz isofrequency contour in AAF. A) is a surface view of cortex indicating the injection site and best-frequency determinations of microelectrode penetrations. The dark-field photograph to the left is of a frontal section taken through the injection site that has been processed for HRP. The white arrows indicate the limit of the reaction product. The dark-field photograph to the right is of a frontal section through the injection site that has been processed for autoradiography. The exposure time of this injection site (and all injection sites) is the same as the exposure time for the sections through the MGB that contain the terminal labelling. B) shows sections processed for HRP numbered rostral to caudal in 120 μ steps. C) shows drawings made from D. D) shows dark-field photographs of adjacent sections to B that have been processed for autoradiography. A comparison of columns B and C shows that the thalamocortical and corticothalamic connections of Dd with the isofrequency contour in AAF are reciprocal. Also, the three-dimensional form of the cell and terminal arrays in the MGB after several injections along an isofrequency contour in AAF are similar to the form of cell and terminal arrays after a single injection in AAF.

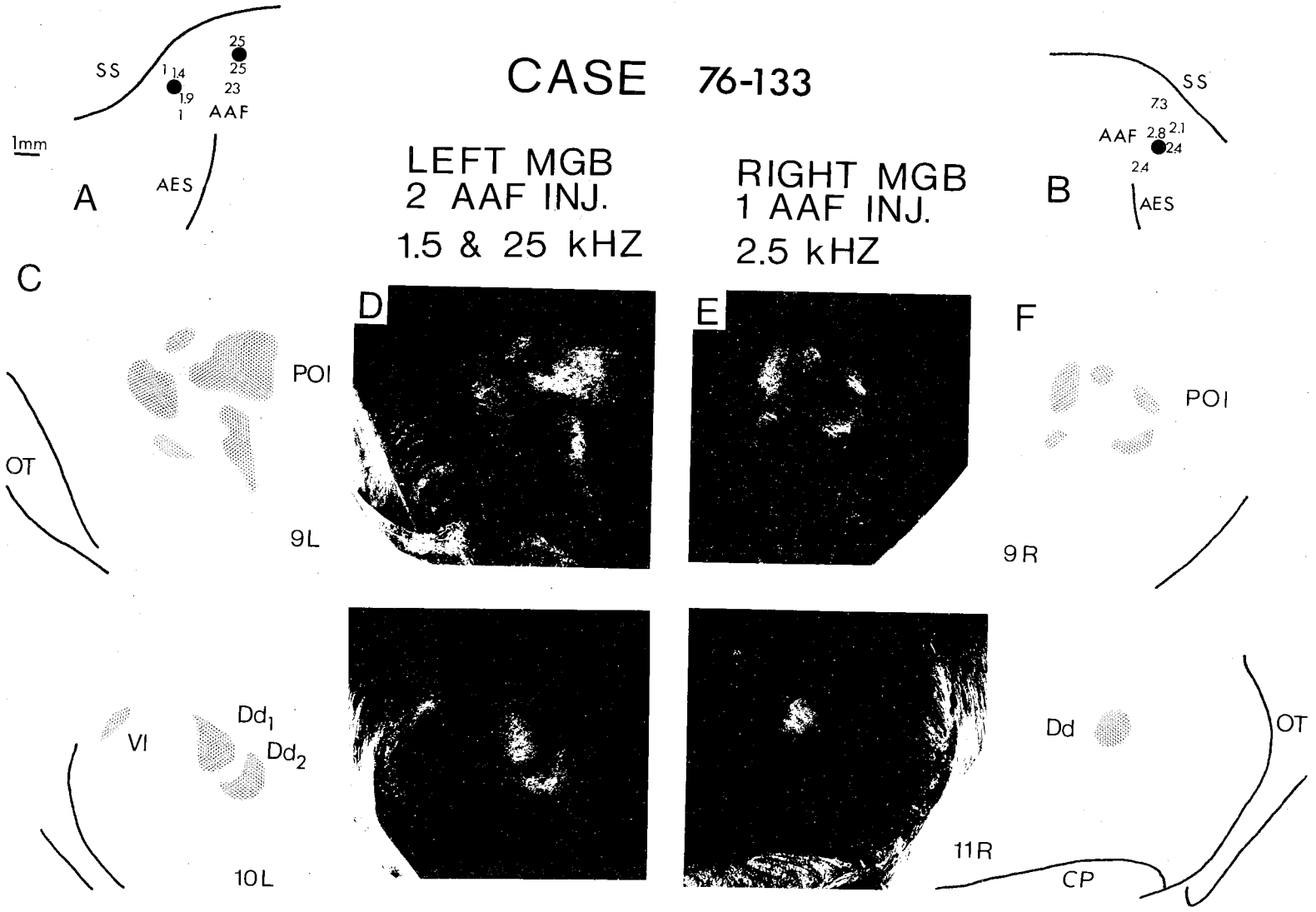
CASE 76-133
LEFT MGB
2 AAF INJ.
1.5 & 25 kHZ
RIGHT MGB
1 AAF INJ.
2.5 kHZ
A
SS
AAF
AES
1mm
25
25
23
1.4
1.9
1
B
SS
AAF
AES
7.3
2.8
2.1
2.4
2.4
C
POl
OT
9L
D
E
F
POl
9R
VI
Dd1
Dd2
10L
Dd
OT
11R
CP

light through the objective under dark-field illumination in a manner typical of fiber bundles cut in cross section. It is thus believed that this lateral label was at least principally of fibers descending to more caudal regions of the MGB.

In the one long survival case, fiber labelling was also noted in the dorsal aspect of the cerebral peduncle. These fibers are probably destined for the pontine nuclei and were situated in the region of the cerebral peduncle where corticopontine fibers of temporal, occipital, and parietal origin are located (Brodal, '69). Also, descending fibers were noted in the brachium of the inferior colliculus (BIC) in the caudal MGB (Fig. 14, sec. 46). These labelled fibers could be followed in the BIC to the inferior colliculus. In slow flow AI cases, fibers were also observed in the BIC in the caudal aspect of the MGB, and these labelled fibers continued within the BIC to the inferior colliculus.

Terminal field labelling in MGB after AII injections of tritiated amino acids

Heavy labelling was observed in the middle and posterior thirds of the MGB after single injections of ^{3}H-l-leucine into AII. The autoradiographic label was of a pattern similar to the HRP label and was noted in the Dc, VL, and M subdivisions of the geniculate body. The heaviest label was over Dc, followed by VL (Figs. 14 and 15).

When following the labelling caudorostrally in frontal sections, above background autoradiographic grains were first seen in the caudal pole of the MGB in Dc. The labelling in Dc has an intricate and complex pattern, with regions of light and heavy label (see Fig. 14, sec. 48 and 50; Fig. 15). More rostrally, the lateral region of the MGB (over pars lateralis and pars ovoidea) was free of label (Fig. 14, sec. 50). At this level, label was recorded in Dc, M, and VL and surrounded the label-free region. Rostral to this level, the label over Dc, M, and VL attenuated.

Reciprocity of thalamocortical and corticothalamic connections

In 10 of these cases, both anterograde and retrograde tracers were injected at single loci in AII. These experiments demonstrated that the projections to and from Dc, VL and M were (with certain reservations) reciprocal (Figs. 14 and 15).

The general strength of labelling of the two tracers in MGB subdivisions coincided. Thus, for both tracers, Dc had the heaviest labelling, followed by VL. Labelling in M was the lightest. Also, regions in Dc where HRP cells were clumped generally had heavier ARG labelling than surrounding areas of Dc (see Fig. 14, sec. 48 and 50).

On the other hand, clear variations in the pattern of label densities of the two tracers were often observed within the MGB subdivisions connected to AII. That is, over some HRP-labelled cell regions within an MGB subdivision, labelling was very dense; over other (even adjacent) labelled cell regions within the same subdivision the corticothalamic projection could be very light (e.g., see Fig. 14, sec. 48; Fig. 15, sec. 10). Thus, the AII corticothalamic and thalamocortical projections were reciprocal in the sense that all HRP-labelled cells were overlain with above background ARG label. However, the relative strength of the ascending and descending connections was commonly regionally variable.

Topographic organization

Examination of several single injection cases revealed no apparent systematic topography of AII projections to and from MGB nuclei.

Fig. 10. A comparison of the pattern of the corticothalamic projections from a single locus in AAF with the pattern of projections from two cochleotopically dissimilar representational positions in AAF. In this experiment, .2 μl injections of HRP and ^{3}H-l-leucine (2 μC) were made at 1.5 and 25 kHz loci in the left AAF and at a 2.5 kHz locus in the right AAF. A and B are surface views of the left (A) and right (B) cortices and indicate the positions of the best-frequency determinations and injections. D shows dark-fields of the left thalamus; 9L is taken through POl and 10L through the rostral MGB. C shows drawings made from D. The stippling indicates above background ARG labelling. E (and F) are sections taken from the same level as D (and C) of the right MGB. Note the topographic organization of the projection in section 10L with Dd_1 corresponding to the projection from the higher frequency locus in AAF and Dd_2 corresponding to the lower frequency place projection. Also, the complex topographic projection from a single locus in AAF to POl is to several distinct cell groups in POl (section 9R). This general pattern in POl does not change, but each component appears to expand in area after two injections at dissimilar cochleotopic representational positions in AAF (section 9L).

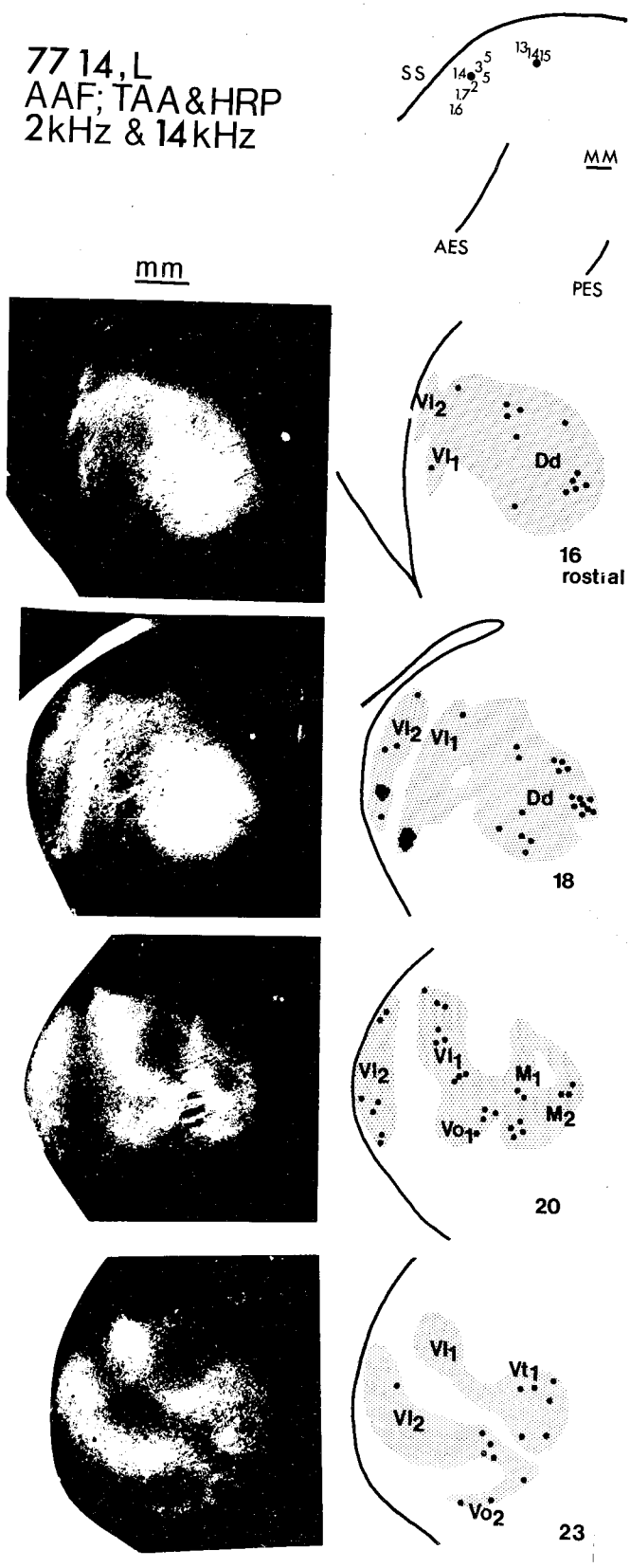
77 14, L
AAF; TAA & HRP
2kHz & 14kHz
SS
13 14 15
14 3 5
1,7 2
16
MM
AES
PES
mm
VI2
VI1
Dd
16
rostral
VI2
VI1
Dd
18
VI2
VI1
M1
M2
Vo1
20
VI1
Vt1
VI2
Vo2
23

In these cases, injections were made at various positions along the rostrocaudal dimension of the field with respect to the cochleotopic organization of AI. Also, in these cases, injections were made from sites near the AI-AII border to positions about 2.5 mm ventral to AI.

In one case, two injections were made in AII at different loci. Both were about 1 mm from the AI-AII border, one being ventral to the site of representation of 2 kHz in AI, and the other ventral to the site of representation of 11 kHz (Fig. 15). There was no obvious difference between MGB labelling in this case when compared to single injection cases.

The connections of restricted AII loci with Dc invariably occupied large regions of this nucleus. Each locus in AII gave and received projections to and from several apparently separated regions within Dc (Fig. 14, 15, and 16). However, the entire nucleus is never occupied by either label after single AII injections (Fig. 14, 15, 16, and 17). Thus, there may be at least some crude systematic topography of this complex projection.

The AII connections in relation to AI connections

An examination of the AII connections with the MGB indicated that AII did not give or receive projections from several regions of the MGB to which AI is connected. To test this observation directly, the two-tracer paradigm was again employed to compare the AII and AI projection arrays. In these studies, anterograde tracer was again introduced at restricted AI loci; and retrograde tracer at restricted AII loci. The data presented here were from four such AI and AII injection experiments.

The results indicated that most of the AII projection arose from regions of the MGB caudal to the thalamic origins of the AI projection (Fig. 16, sec. 22–26). Label in this exclusive caudal region was contained within the Dc. Proceeding rostrally, when the AI projection did begin, the ventral division components of that projection fell within the label-free region of the AII projection (Fig. 16, sec. 21 and 20; Fig. 17). The Dc component of the AII projection at this level appeared just dorsal to the AI projection to pars lateralis (Fig. 16; Fig. 17). The VL component bordered the AI projection to pars ovoidea ventrally (Fig. 16; Fig. 17).

Thus, AI and AII appear to have largely separated projection arrays with AI interconnected with the middle and anterior thirds of the MGB and AII interconnected with the posterior and middle thirds. In the middle third, there is an overlap of the two reciprocal projections which is restricted to the medial division.

DISCUSSION

Major conclusions of this study include the following: 1. Any restricted AI locus receives input from a folded sheet of neurons passing through pars lateralis, pars ovoidea, and the "transitional zone" of the ventral division, from a column of neurons extending rostrocaudally through the deep dorsal nucleus of the dorsal division and the medial division, and from neurons in the lateral division of the posterior group. 2. AAF receives inputs from these same nuclei, with the same basic pattern of thalamocortical projection. However, unlike the projection to AI, the projection to AAF from the ventral division arises from a very sparse and discontinuous array of neurons. 3. Projections from all of these nuclei to AI and AAF are systematically topographic and appear to be cochleotopically ordered. 4. AII receives projections from a different group of thalamic nuclei than AI and AAF. The projection to AII originates from the caudal dorsal nucleus, the ventrolateral nucleus, and the medial nucleus (which also projects to AI and AAF.) 5. Corticothalamic projections from

Fig. 11. A representative example of the topographic order of the corticothalamic and thalamocortical connections with respect to the cochleotopic organization of AAF. In this experiment, the left AAF was injected at 2 and 14 kHz loci with .1 μl of HRP and ^{3}H-l-leucine. The surface view of the cortex indicates the injection loci and recording data. The dark-field photographs on the left are of sections that have been processed for both HRP and autoradiography. These sections have been redrawn on the right. Each dot represents an HRP-granule-containing cell and the stippling indicates autoradiographic labelling that is above background. The projections are topographically organized and denoted by a subscript: 1 corresponding to the label resulting from the 14 kHz place injection and 2 from the 2 kHz place injection. The sections are numbered rostral to caudal in 200 μ steps. The exposure time for autoradiography was unusually long (4.5 months). Also, the dark-field photomicrographs have been underexposed to show better the light ARG labelling in the ventral division. The fact that all HRP-labelled cell arrays are overlain by above background autoradiographic labelling indicates a degree of reciprocal connectivity.

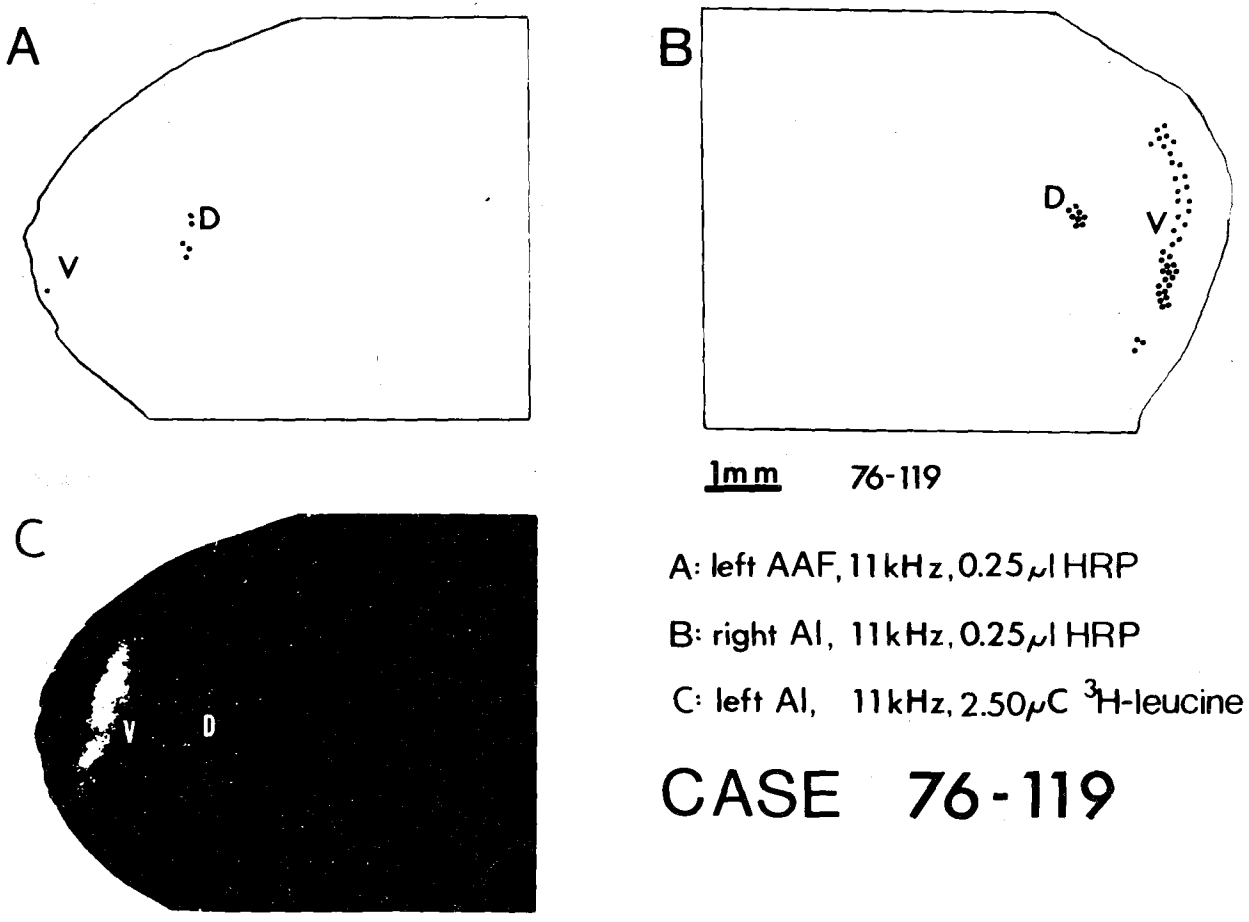

Fig. 12. An example in which the connections of AI and AAF with the MGB are compared directly in a single cat. In this experiment, the left AI cortical field was injected with .25 μl (2.5 μC) of ^{3}H-l-leucine at an 11 kHz locus, the left AAF was injected with .25 μl of HRP at an 11 kHz locus, and the right AI was injected with .25 μl of HRP at an 11 kHz locus. Section A represents the AAF thalamocortical projection; section B represents the AI thalamocortical projection; and section C represents the AI corticothalamic projection. All sections are taken from the same level of the MGB. A comparison of sections B and C indicates that the AI projection is reciprocal. Comparison of sections A and C indicates that AI and AAF give and receive projections from the same region of the Dd nucleus. Comparison of A and B indicates that the thalamocortical projection from Vl to AAF is sparser than the projection from Vl to AI.

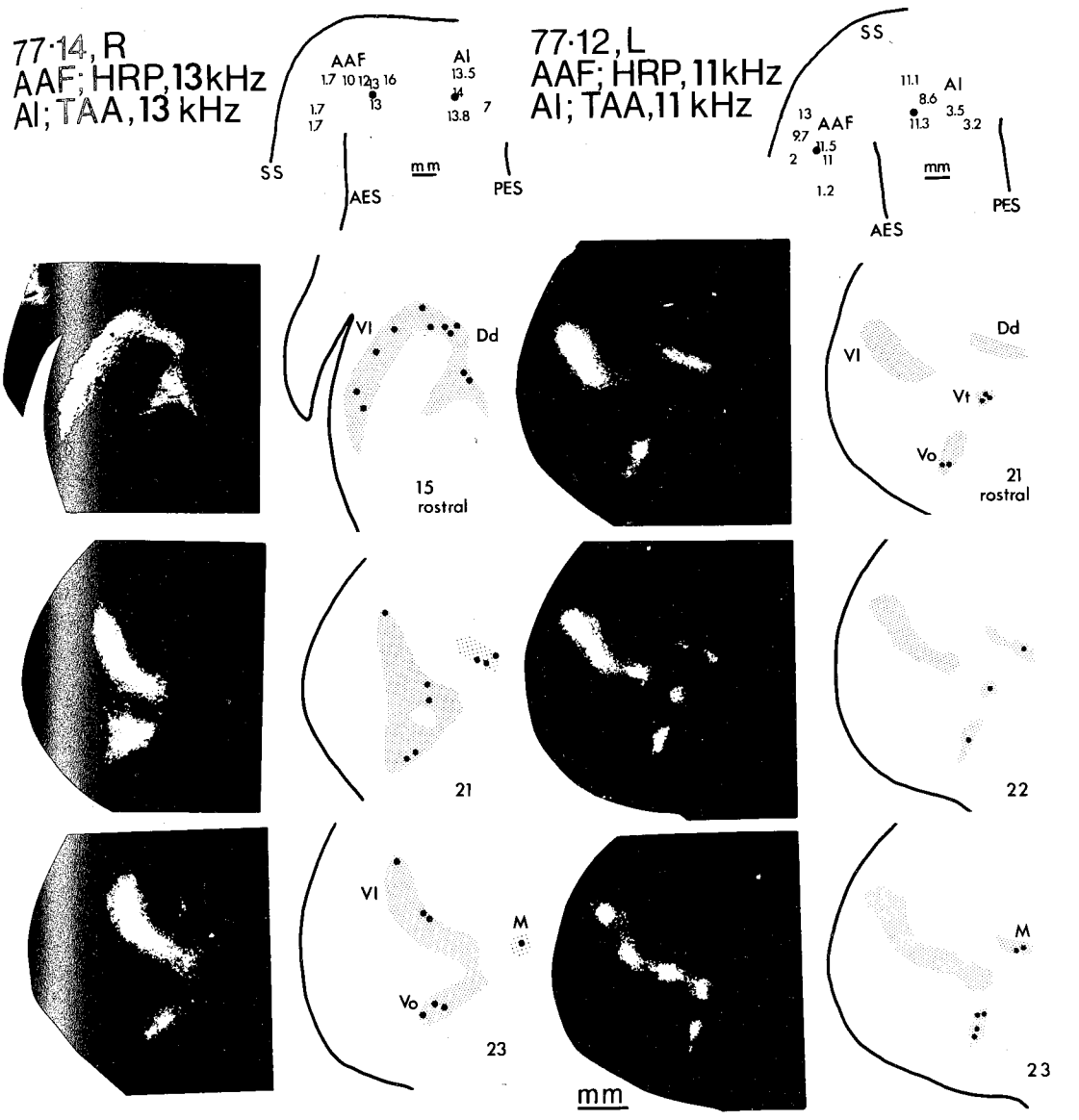

Fig. 13. Two examples of a direct comparison in single hemispheres of the connections of cochleotopically homotypic loci in AI and AAF with the MGB. In the experiment on the left of this figure, .15 μl of HRP was injected into AAF at a 13 kHz locus and .15 μl of ^{3}H-l-leucine was injected into AI at a 13 kHz locus. The sections on the left have been processed for both HRP and autoradiography and are photographed with dark-field illumination. These sections have been redrawn on the right. Each dot represents an HRP-granule-containing cell and the stippling indicates regions of autoradiographic labelling. In the experiment on the right, .2 μl of HRP were injected at an 11 kHz locus in AAF and .1 μl (2 μC) of ^{3}H-l-leucine was injected at an 11 kHz locus in AI. Again, the sections have been processed for both autoradiography and HRP and are redrawn on the right. The similarity of the AI and AAF connections to MGB are apparent. Sections in these two experiments are numbered rostral to caudal in 200 μ steps.

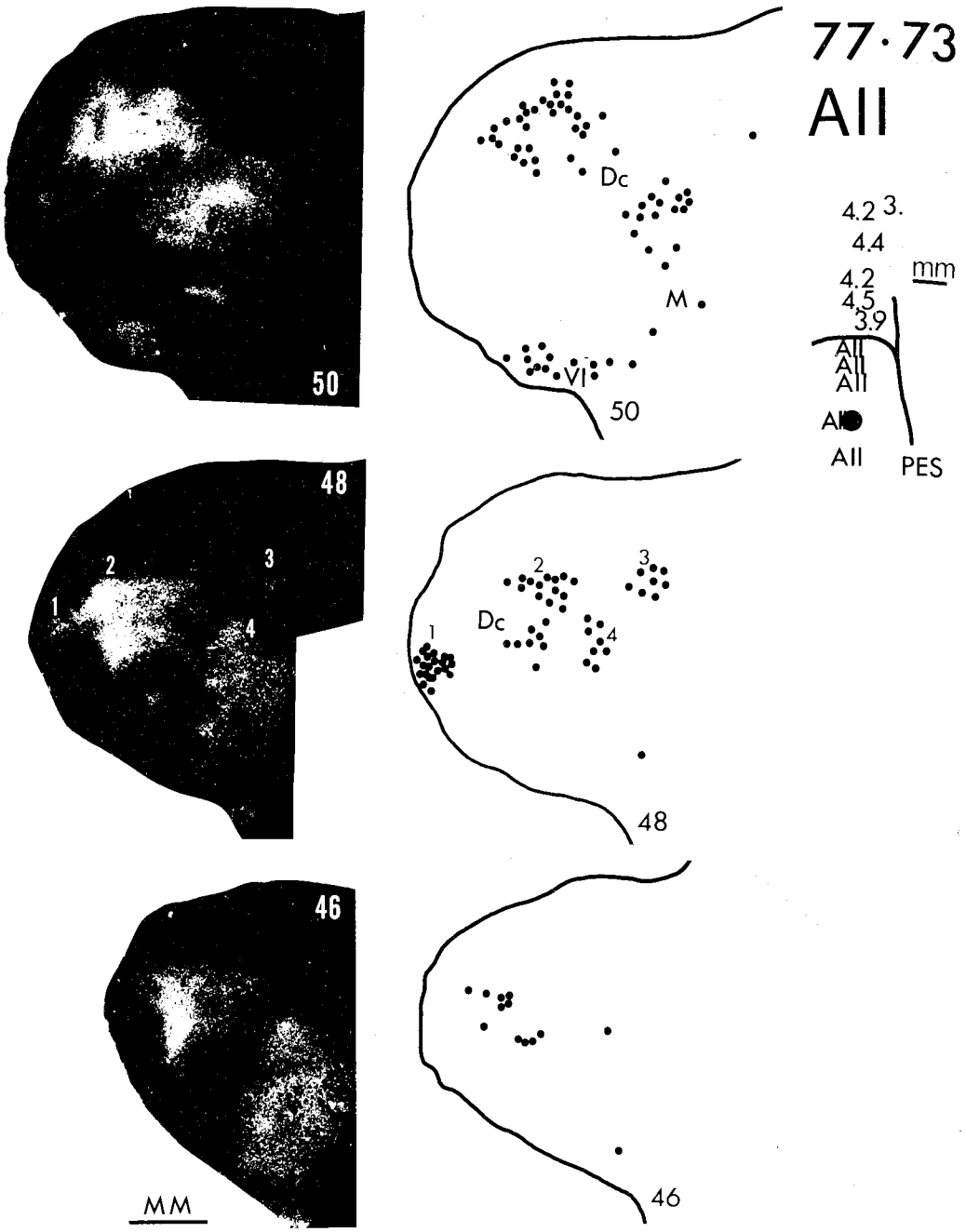

Fig. 14. An example of the corticothalamic and thalamocortical connections of a locus in AII with the MGB. In this experiment, an injection of .25 μl of ^{3}H-l-leucine and an injection of .3 μl HRP (7 days later) were made at the same locus in AII. (Total survival time for autoradiography was 8 days.) The surface view of the cortex at the right shows the position of the injection site in AII with respect to the functional organization of AI. The numbers indicate the best-frequency determinations of penetrations into AI. "AII's" indicate the position of penetrations where broad-frequency responses of units and unit clusters indicative of the AII field were noted. The dark-field photographs on the left are of sections processed for autoradiography; the sections drawn on the right are of adjacent sections processed for HRP. Section 50's are taken from the caudal aspect of the middle third of the MGB, section 48's from the caudal third of MGB, and section 46's from the posterior pole of the caudal third of the MGB. The numbers in the adjacent section 48's indicate four subregions of Dc that contain both dense groups of labelled HRP-granule-containing cells and distinct areas of more intense autoradiographic labelling. For all sections, there is a general coincidence of the spatial disposition of the two labels. This is especially true considering that adjacent sections are being compared and that the ARG-processed sections are more shrunken than the HRP sections. An exception to this overlap of tracers is the labelled BIC fibers in the ventromedial region of section 46. Sections are numbered caudal to rostral in 360 μ steps.

these three cortical fields are all (with reservations outlined earlier) reciprocal. 6. There is a segregation of the reciprocal connections between the caudal half of the ventral division and AI into periodic parallel bands. This periodic banding was also noted in the corticothalamic projections of AAF onto the caudal aspect of the ventral division.

Relation to previous studies of MGB-auditory cortical field interconnections

AAF

Since AAF has only recently been discovered (Merzenich et al., '75, Knight, '77), no previous direct connectional studies have been conducted in this field. However, the connectivity of the dorsal aspect of the anterior ectosylvian gyrus, in the approximate region of the location of AAF in most cats, has been considered in several previous studies. Rose and Woolsey ('58) found that the posterior group of the thalamus was preserved after cortical ablations that included most of the auditory cortex. However, when the ablation was extended to SII and included the general region of AAF as well, the anterior region of the posterior group (POl) degenerated. Waller recorded retrograde degeneration in the rostral aspect of the small-celled region (principal division, probably Vl) of the MGB after a lesion restricted to the dorsal part of the anterior ectosylvian gyrus (probably AAF). A lesion possibly restricted to the region of AAF produced scanty anterograde degeneration in the magnocellular division (Pontes et al., '75). Lesions at various MGB loci produced anterograde degeneration undoubtedly extending across AAF in the study of Wilson and Cragg ('69). Lesions restricted to the "principal division" (probably Vl) also produced degeneration almost certainly extending into AAF in the studies of Niimi and Naito ('74); this degeneration was less pronounced than that recorded in AI. Thus, there is no general agreement between the various studies as to what the connections of the dorsal aspect of the anterior ectosylvian gyrus are with the auditory thalamus. However, taken together, these earlier data indicated that AAF probably received projections from POl, was reciprocally connected to Vl, and projected onto the medial division. Thus, as a composite, they are consistent with some of the results of the present study of the connections of AAF.

AII

Lesions in AII alone produced little or no retrograde degeneration in the MGB (Rose and Woolsey, '49; Diamond et al., '58). Anterograde degeneration studies indicated that AII projected to the caudal pole (Dc) of the MGB, as well as to other components of the dorsal division (Pontes et al., '75). Diamond et al. ('69) reported that AII lesions produced the same pattern of anterograde degeneration as AI lesions; however, their lesions almost certainly encroached upon AI or upon one of the other cochleotopically organized cortical fields bordering AII. Lesions of the caudal pole (Dc) of the MGB produced anterograde degeneration in AII (Sousa-Pinto, '73; Niimi and Naito, '74), and HRP injections in AII produced labelled cells in the "caudal," dorsal, and magnocellular divisions (Winer et al., '77). Finally, TAA injections into AII produced autoradiographic label in the caudal pole of the MGB (Dc), VL, "magnocellular part," and superficial dorsal and deep dorsal nuclei (Pontes et al., '75).

Thus, several of these studies are in agreement with the observation that AII gives and receives projections from the caudal pole of the MGB, which is consistent with the observations of reciprocal connections of AII with Dc reported in the present study. The reports of thalamocortical (Winer et al., '77) and corticothalamic (Pontes et al., '75) connections with the "magnocellular" region presumably correspond to the reciprocal connections with the medial division observed in this study. There is only one report of a corticothalamic projection to VL (Pontes et al., '75) and no report of a VL thalamocortical projection. Other reported connections probably reflect problems inherent in the experiment protocols that were used (see below).

AI

The connections between AI and the thalamus of cat have been extensively studied with the techniques of Marchi degeneration (Woollward and Harpman, '39; Ades, '41), retrograde degeneration (Mettler, '32; Rose and Woolsey, '49; Neff et al., '56; Diamond and Neff, '57; Rose and Woolsey, '58; Diamond et al., '58; Locke, '61; and Jones and Powell, '71), anterograde degeneration after lesions in the MGB (Wilson and Cragg, '69; Sousa-Pinto, '73; Niimi and Naito, '74), anterograde degeneration after lesions in AI (Rasmussen, '64; Kasama et al., '66; Diamond et al., '69; Van Noort, '69;

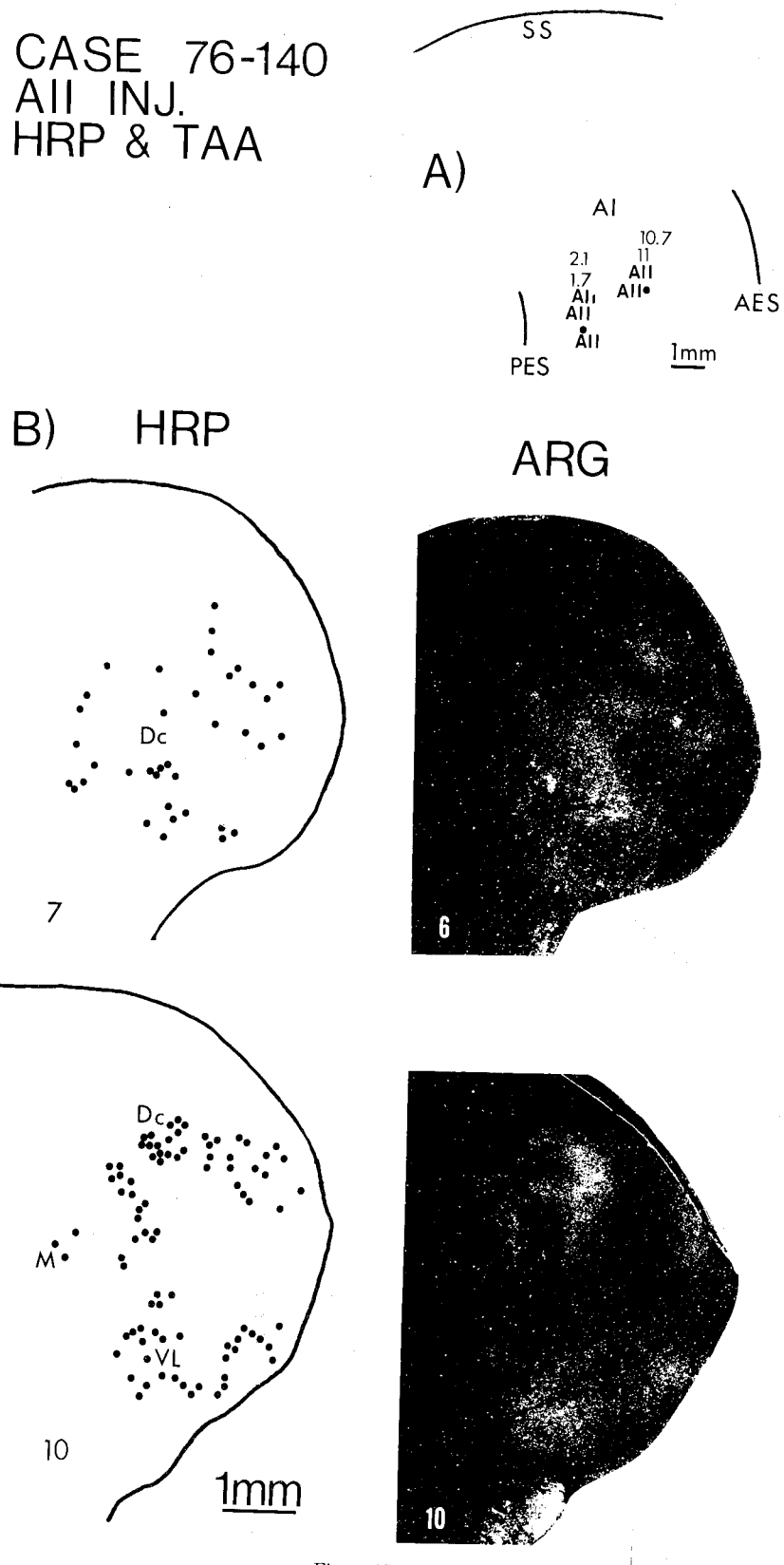
CASE 76-140
AII INJ.
HRP & TAA
SS
A)
AI
10.7
11
2.1
1.7
AII
AII
AII
AII
AII
AES
PES
1mm
B) HRP
ARG
Dc
7
6
Dc
M
VL
10
1mm
10

Figure 15

Jones and Powell, '71; Pontes et al., '75), retrograde axonal transport methods (Winer et al., '77; Colwell and Merzenich, '80), and anterograde axonal transport methods (Pontes et al., '75; Colwell and Merzenich, '80). Retrograde degeneration was found to be quite extensive in the rostral half of MGp after AI lesions, but little or no degeneration was noted in MGm (Rose and Woolsey, '49, '58; Neff et al., '56; Diamond and Neff, '57; Diamond et al., '58; Locke, '61). Lesions to MGp, and particularly to Vl, produced anterograde degeneration in large regions of auditory cortex (Wilson and Cragg, '69; Niimi and Naito, '74); however, the degeneration in cortex always appeared heaviest in the region of AI (Sousa-Pinto, '73; Niimi and Naito, '74). These results are probably a reflection of the strong thalamocortical projection of Vl to AI.

After lesions in AI, anterograde degeneration was recorded in MGp (Kasama et al., '66; Van Noort, '69), MGm, and POl (Jones and Powell, '71). Diamond et al. ('69) and Pontes et al. ('75) noted degeneration in Vl, Vo, Dd, and the "magnocellular" division (which probably includes the medial division). Tritiated amino acid injections into AI produced labelling in these same subdivisions of the MGB (Pontes et al., '75; Colwell and Merzenich, '80). HRP injections in AI produced labelled cells in the ventral, dorsal, and medial divisions of MGB and in the regions of the posterior group (Winer et al., '77; Colwell and Merzenich, '80).

New observations

The above brief review of the connectional literature indicates that there is general agreement between the present findings and those reported previously in terms of the subdivisions of the MGB that are interconnected with AI and auditory cortex caudal to AI (AII). By using the more refined techniques of combined microelectrode mapping/axonal transport tracing, the present work extends knowledge about the organization of the auditory thalamocortical system. New observations include: 1) a description of the connections of the anterior auditory field; 2) the observation of a topographic, and probably cochleotopic, organization of connections of both AAF and AI with all four of the major subdivisions of the MGB to which they are connected (a similar topographic order for AI has been reported by Colwell and Merzenich ('80) using similar techniques); 3) the folded sheet configuration of connections of the ventral division with single cortical loci in AAF and AI (also noted by Colwell and Merzenich for AI connections); 4) the description of a banded segregation of connections along the folded sheet configuration of the ventral division (see also Colwell and Merzenich, '80); 5) the direct visualization of the spatial relationships of the reciprocal connections between AII and AAF with the MGB; 6) the direct visualization in individual cats of the precise spatial interrelationships of the AI, AII, and AAF connections with the MGB.

These observations were made possible by several attributes of the protocol selected for this study. The use of the microelectrode mapping techniques established the functional architecture of the auditory cortex in individual cats prior to the injection of anatomical tracers. In previous investigations, the sulcal patterns of the cat cortex and the evoked-potential maps of Woolsey ('60) were usually used to determine the position of the cortical fields. However, the position of auditory cortical fields in relation to the sulcal patterns varies from animal to animal (Merzenich et al., '75, '77). Moreover, the cortical field maps of Woolsey have been revised as a result of new data obtained from microelectrode mapping studies (Merzenich et al., '75; Merzenich et al., '77). Thus this technique allowed us to determine the connections of the anterior auditory field, a cortical field whose anterior aspect had previously been assigned to AII and whose remaining posterior aspect had been assigned to AI. By this method we were also able to determine the topography of connections for the cochleotopically organized cortical fields. By identifying the boundaries of the auditory cortical fields we were confident that the connections that were observed arose

Fig. 15. In this experiment, .15 μl of a mixture of HRP and ^{3}H-l-leucine was injected at two different loci in AII. A) indicates the position of the two injections. Both were made about 1 mm from the AI-AII border, at referenced positions of 2 and 11 kHz with respect to AI. B) shows adjacent sections processed for HRP (left) and autoradiography (right). Numbering is caudal to rostral in 200 μ steps. Note that any topography of connectivity with respect to the two injection sites is difficult to discern within this complex projection pattern. The two patterns of HRP and ARG label are, in general, similar. However, within subregions of a thalamic nucleus there is often a variation in the densities of distribution of the two tracers (for instance, Dc of section 10).

CASE 77-1
AI; ARG;
6 kHZ INJ.
AII; HRP

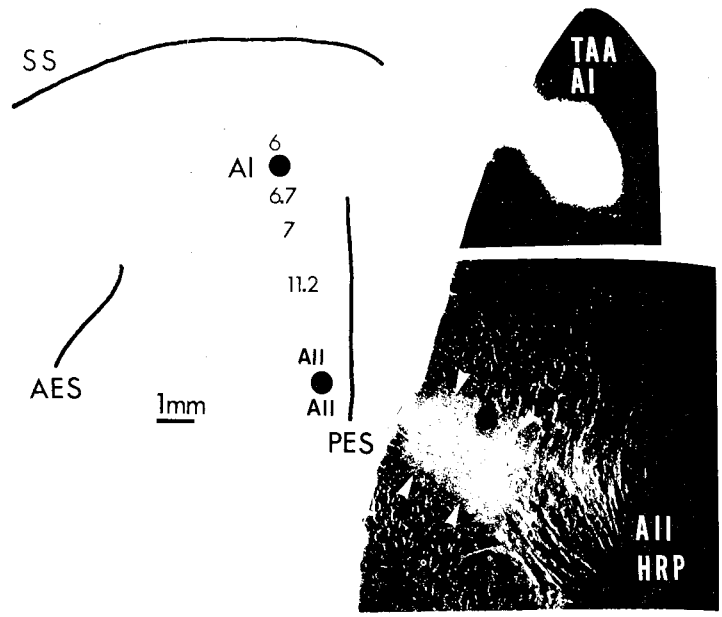

AII; HRP

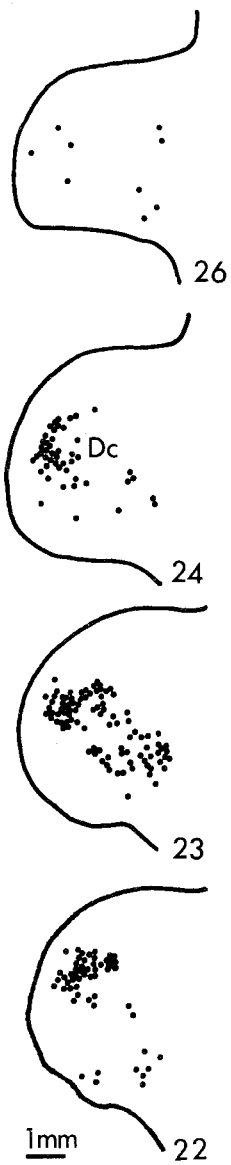

AII; HRP AI; ARG

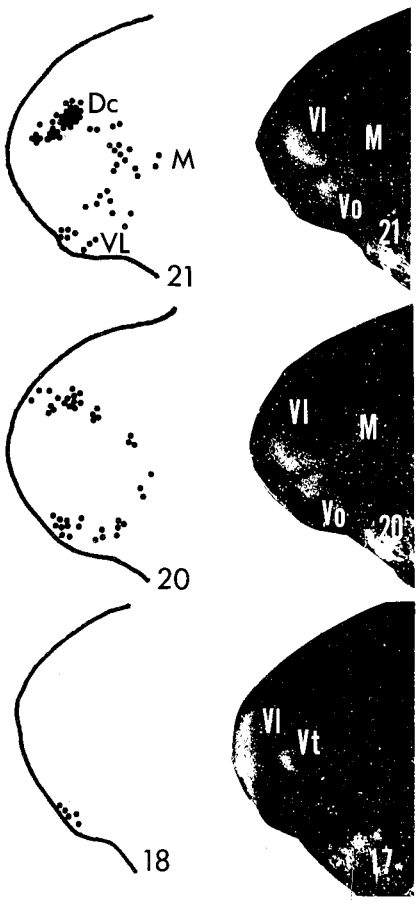

only from single cortical fields; there was no spillage of tracer into adjoining cortical fields.

Other attributes of the protocol adopted were the Golgi-like labelling of proximal dendrites with large HRP injections and the use of the two-tracer/two-field protocol; these two techniques insured the proper MGB subdivision assignation of the observed neuronal and terminal arrays. This approach was important since there is difficulty in determining the subdivisions of the MGB of the cat based entirely on Nissl architecture (Morest, '64; Oliver and Hall, '78). In the past, different investigators used different parcellations of the MGB based on the work of Rioch ('29) (Nissl cytoarchitecture) or Morest ('64) (Golgi cytoarchitecture) or combinations of these two systems of parcellation. The approach adopted here helped to integrate these two views.

The corticothalamic and thalamocortical fiber paths are different

The corticogeniculate fibers pass from injection sites in all three studied fields into the internal capsule. They pass ventral to the LGN and through the reticular nucleus of thalamus to enter the auditory dorsal thalamus. These observations are in general agreement with those of Diamond et al. ('69). It is of interest to note that this corticothalamic pathway is apparently different from the path of thalamocortical fibers (Woollard and Harpman, '39; Sousa-Pinto, '73). The thalamocortical fibers traverse the putamen or pass around it. They pass dorsal, caudal, or posterior to the claustrum (but not through it) to reach the auditory cortex. Thus, the geniculocortical pathway is ventral and lateral to the corticogeniculate pathway.

Each cortical field is interconnected with several nuclei in the thalamus

In previous studies, the argument has been that either each auditory cortical field is connected to several subdivisions of the MGB (Diamond et al., '69; Winer et al., '77) or that each cortical field is connected to only one thalamic subdivision (Sousa-Pinto, '73; Pontes et al., '75). In these experiments, electrophysiological mapping prior to the injection of tracers insured that the tracers did not diffuse into adjacent cortical fields. Thus, it is certain that AI, AII, and AAF each receive projections from and project to several subdivisions of the MGB.

Although every field receives projections from several subdivisions of the MGB, each studied cortical field also has a single different subdivision to which it is most strongly connected. The same conclusion has been made by Winer et al. ('77). Thus, AI is most strongly interconnected (thalamocortically and corticothalamically) to pars lateralis, AAF to the deep dorsal nucleus, and AII to the caudal dorsal nucleus.

AI, AII, and AAF are parallel auditory processors

Each of the cortical fields studied has strong and direct connections with the MGB. The electrophysiological recordings in these fields indicate that they are activated by auditory stimuli with approximately the same latencies. These two lines of evidence demonstrate that AI, AII, and AAF are processing auditory information in parallel.

Essential and sustaining projections

To explain the results of their retrograde lesion studies, Rose and Woolsey ('49, '58) proposed the concepts of "essential" and "sustaining" thalamocortical projections. An "essential" projection from a thalamic nucleus to cortex existed if destruction of one cortical field produced marked degeneration in the nucleus. A "sustaining" projection was present if destruction of either of two cortical areas produced little or no degeneration in a tha-

Fig. 16. An example of direct comparisons made, in single hemispheres, of the connections of AI and AII with the MGB. In this experiment, .2 μl of ^{3}H-l-leucine (2 μC) was injected at a 6 kHz locus in AI and .2 μl of HRP was injected into AII about 1 mm ventral to the AI-AII border. The surface view of the cortex in the upper part of the figure indicates the positions of the injection sites. The dark-field photomicrographs on the right are of frontal sections through the tritiated amino acid (TAA) and HRP injection sites. The sections on the left, in the lower part of the figure, have been processed for HRP, with each dot representing an HRP-containing neuron. These HRP sections indicate the pattern of the AII thalamocortical projection and the general pattern of the AII corticothalamic projection. The adjacent sections on the right are dark-field photographs of the caudal extent of the AI corticothalamic projection. (Bright areas over the cerebral peduncle, in the region of the section numbers, are due to the reflection of light from the fiber tract, not ARG labelling.) Since AI is reciprocally connected to the MGB, this also indicates the caudal extent of the AI thalamocortical pattern. Note that the connections of the two cortical fields with the MGB are largely segregated, the exception being the medial division. Sections are numbered rostral to caudal in 200 μ steps.

lamic nucleus, while destruction of both areas together produced marked degeneration. There are several possible explanations for the sustaining projection results. Rose and Woolsey ('58) favored the idea that cells of several thalamic nuclei send collateral axons to more than one auditory field and that any set of these collaterals can maintain the integrity of the cells.

These present results are in some respects consistent with the collateral projection concept. All of the cortical fields which sustain

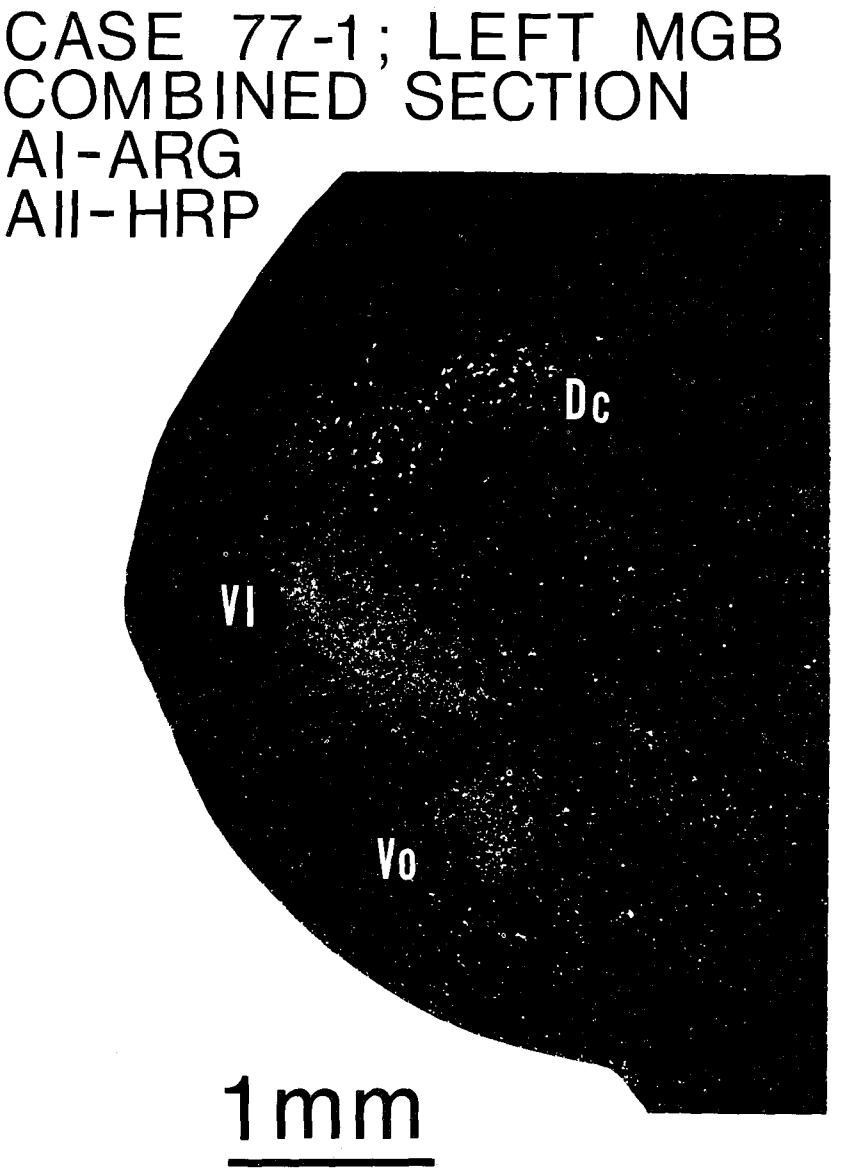

Fig. 17. This dark-field photomicrograph is of a section from the experiment in Figure 16, and has been processed for both ARG and HRP. Autoradiographic label, representing the structure of the AI connections, is apparent in the ventral division (Vl, Vo). A group of HRP-containing cells, representing the structure of the AII connections, is apparent in the caudal dorsal division, just dorsal to Vl. That the two labelling patterns in the ventral and dorsal divisions are segregated is apparent in these dually processed sections.

an MGB subdivision are interconnected with it (see Fig. 18). AAF and AI are both connected to POl, and both these cortical fields had to be lesioned to cause POl to degenerate (Rose and Woolsey, '58; see Fig. 18B). The caudal dorsal nucleus is reciprocally connected to AII and "temporal" cortex (T) (Diamond et al., '69; Cranford et al., '76; Winer et al., '77; see Fig. 18C). Both these cortical fields must be lesioned for Dc to degenerate (Diamond et al., '58; Rose and Woolsey, '58). The medial division, which appears to be connected to every auditory cortical field including AI, AII, AAF, VPAF, T (Diamond et al., '69; Winer et al., '77), and PAF (FitzPatrick et al., '77; see Fig. 18D), only degenerated after all of the auditory cortex had been destroyed (Rose and Woolsey, '58; Diamond et al., '58; Locke, '61).

On the other hand, lesions to AI caused the complete degeneration of the rostral aspect of the principal division (Rose and Woolsey, '49, '58; Diamond, '58). However, the ventral division, which comprises this region of the MGB, is connected to at least four cortical fields: AI and AAF, VPAF (Andersen, '79), and PAF (FitzPatrick et al., '77). Thus, AI is clearly not a singular destination for ventral division fibers, as the most simple interpretation of an "essential" projection might suggest.

The topography of connections of AI and AAF reflects the cochleotopic organizations of the projecting and target nuclei

There is a systematic variation in the order of connections between AI and AAF and the nuclei of the MGB. The topographies of these connections, when compared with the cochleotopic organizations observed in electrophysiological recording experiments in Vl of cat (Aitkin and Webster, '72; Aitkin, '73; Rose and Woolsey, '58) and Dd of squirrel monkey (Gross et al., '74), are consistent with the interpretation that loci in these two cortical fields are interconnected with cochleotopically homotypic regions of at least these MGB nuclei and probably all the MGB nuclei to which AAF and AI are connected.

Two-systems hypothesis

Although each cortical field examined had, overall, a unique pattern of connectivity, two basic patterns of connectivity were recorded (see Fig. 19). One pattern of connectivity is limited mostly to the rostral aspect of the MGB. This pattern is comprised of the morphologically laminated nuclei of the ventral division (Vo and Vl) laterally and Dd and M medially, and may also include POl. The cortical fields exhibiting this pattern of connectivity include AI, AAF, and VPAF (Andersen, '79), and probably PAF (FitzPatrick et al., '77). Since these projecting thalamic nuclei and cortical fields share the common feature of being cochleotopically organized (with component neurons commonly sharply "tuned"), this pattern of connectivity will be referred to as the "cochleotopic pattern" or "cochleotopic system" (see Fig. 19).

The second pattern of connectivity is exemplified by the connections of AII. The AII cortical field gives and receives projections from the more caudal aspects of the MGB. AII is connected to the Dc, VL, and M subdivisions of the MGB. The two-tracer/two-field experiments demonstrated that the connections of some of the "cochleotopic pattern" fields (AI and AAF) with the MGB and the connections of AII with the MGB are largely segregated,

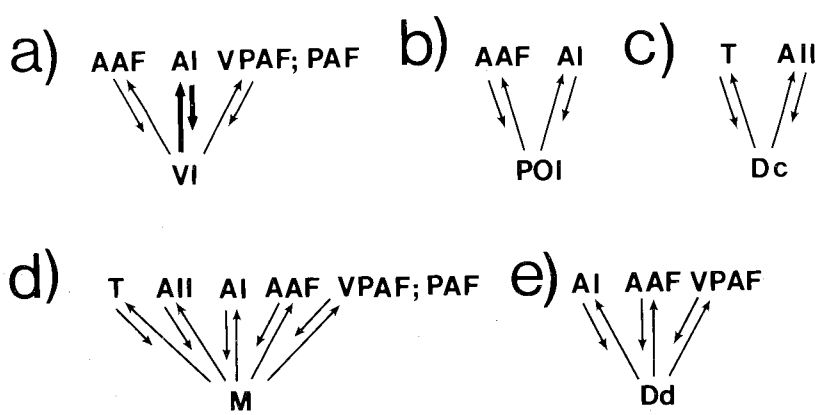

Fig. 18. The reciprocal connections of the various subdivisions of auditory thalamus with several cortical fields as elucidated by this study, Diamond, et al. ('58), Diamond et al. ('69), and FitzPatrick et al. ('77).

with the only overlap occurring in the medial division of the MGB (M). Previous studies indicate that the "temporal" region of cortex gives and receives projections from the MGB in a pattern similar to the AII connections (Cranford et al., '76; Diamond et al., '58; Winer et al., '77; Diamond et al., '69; Waller, '40). (The insular region does not appear to be directly connected to the MGB according to Winer et al.) Since AII and T have broadly tuned neurons, indicating that they receive convergence from a large sector of the cochlear sensory epithelium, this pattern of connections will be referred to as the "diffuse pattern" or "diffuse system" (see Fig. 19).

Thus, there appear to be two functionally distinct and largely segregated systems connecting MGB subdivisions and auditory cortical fields. The cortical fields of the "cochleotopic system" include AI, AAF, PAF, and VPAF. The cortical fields of the "diffuse system" include AII and the "temporal" cortical field.

Two auditory thalamocortical systems have been previously reported. Rose and Woolsey ('58) and Diamond et al. ('58) noted that destruction of AI (as defined by Woolsey and Walzl, '42) produced extensive retrograde degeneration in the anterior aspect of pars principalis of the MBG, whereas lesions ventral to AI (AII and "temporal" cortex) produced retrograde degeneration in the caudal pole of the MGB. These and other observations led Rose and Woolsey ('49, '58) to propose the division of "essential" thalamocortical projections to AI and "sustaining" projections to areas surrounding AI. Two general systems of thalamocortical connections have been reported by others in the cat (Winer et al., '77; Graybiel, '73) and the treeshrew (Casseday et al., '76). These two-system schemes are comprised of a major pathway between the ventral division and AI auditory cortex (the "core" system of Casseday et al., '76 and Winer et al., '77, and the "lemniscal line" system of Graybiel, '73) and a second major pathway between areas of the auditory thalamus surrounding the ventral division and areas of auditory cortex surrounding AI (the "belt" system of Casseday et al., '76 and Winer et al., '77, and the "lemniscal adjunct" system of Graybiel, '73).

The "cochleotopic-diffuse" pathways reported in the present investigation in general correspond to the two-system parcellations of others. The present findings extend the two-system concept in important ways by indicating the following: 1. Both systems of connections are comprised of several functionally defined auditory cortical fields. Previous studies suggested one of the systems (the cochleotopic system) involved only the single auditory cortical field AI. 2. The two anatomical systems of connection correspond to two functionally distinct types of auditory cortical fields. As previously elaborated, the auditory cortical fields of the cochleotopic system are cochleotopically organized and are comprised of neurons with relatively sharp tuning curves, whereas the cortical fields of the diffuse system have neurons with broad tuning curves and an apparently noncochleotopic organization. Irvine and Huebner ('79) have also reported that neurons of the auditory cortex in regions comprising the diffuse system are relatively more broadly tuned. 3. The topographic organization of connections of cortical fields of the two systems are distinct. The topography of connections of cortical fields of the cochleotopic system appears to follow their functional cochleotopic organization, whereas the topography of connections of the diffuse system appears to follow other rules of organization.

The segregation of connections into a cochleotopic system and a diffuse system appears to extend beyond the thalamocortical-corticothalamic loop. There is evidence for two segregated, ascending systems of connection from the IC to the MGB (see Fig. 19). The projection of the central nucleus (in which neurons are sharply tuned; see Rose et al., '63; Merzenich and Reid, '74) onto the medial geniculate is of the same form and systematic topography (i.e., cochleotopic organization) as the thalamocortical and corticothalamic connections of AI (Casseday et al., '76; Kudo and Niimi, '78; Andersen et al., '78). By contrast, the pericentral nucleus (in which neurons are broadly tuned; see Rose et al., '63; Merzenich and Reid, '74) appears to project to Dc and to other regions of the MGB that project to AII (Casseday et al., '76; Kudo and Niimi, '78; Andersen, '79).

Thus, there appear to be two largely segregated and parallel auditory projection systems connecting the IC, MGB, and auditory cortex (Fig. 19). From the ICC, information in the "cochleotopic system" passes to the rostral MGB and is reciprocally connected with the "cochleotopic pattern" cortical fields. The topographic organization of connections remains consistent with the recorded cochleotopic organization of the IC, MGB, and cortical fields throughout this ascending system.

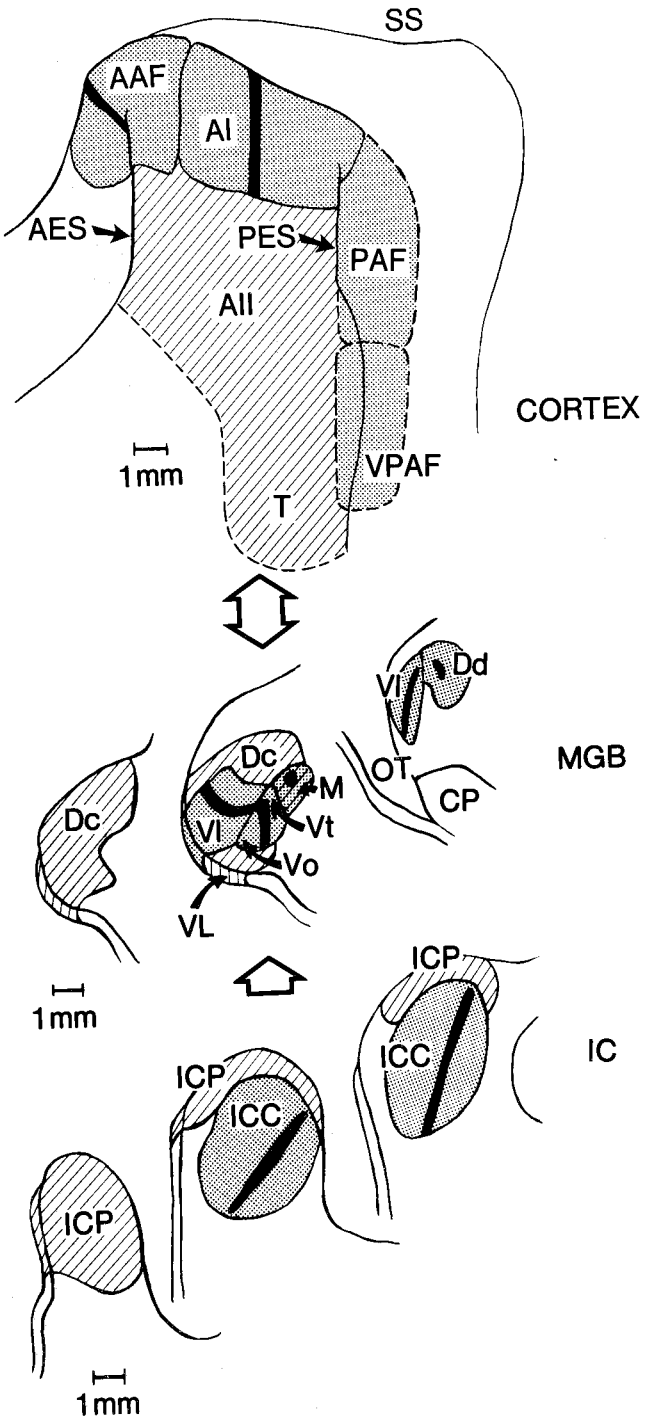

Fig. 19. Schematic diagram of the spatial organization of the diffuse and cochleotopic systems. The top illustration is of the cortical surface. The middle drawings are of frontal sections through the posterior (left), middle, and anterior (right) thirds of the MGB. The bottom sections are through the posterior (left), middle, and anterior (right) thirds of the IC. Arrows between the levels represent the direction of connection. Stippling indicates the areas comprising the cochleotopic system and lines the areas of the diffuse system. The black regions within the cochleotopic system indicate the divergent and convergent forms of connections of discrete loci with the other levels.

From the ICP, information in the "diffuse system" passes to caudal regions of the MGB that are exclusively and reciprocally connected to the "diffuse system" cortical fields. The topographic order of the diffuse system cortical fields with the MGB is complex and not indicative of a simple cochleotopic order.

Divergent-convergent form of projection

One interesting feature of these results is the geometric forms of the projections. Thus, single loci in AAF and AI receive *convergent* projections from sheets and columns of neurons in the MGB and give divergent projections to the MGB in the form of sheets and columns of terminals. Along the connectional sheet in the ventral division, there is also the added complexity of discontinuities in the thalamocortical and corticothalamic projection arrays.

An interesting feature of the sheet and column geometries of these connections is that they appear to reflect the form of the isofrequency contours within Vl (Rose and Woolsey, '58; Aitkin and Webster, '72). It is quite probable that the forms of the connectional arrays in Vo, Vt, Dd, and M also reflect the forms of isofrequency contours within these MGB nuclei which have not yet been functionally mapped in three dimensions. Since multiple injections along isofrequency contours in AAF or AI produced the same general divergent and convergent sheet and column labelling in the MGB as was obtained with single injections, it is probable that all sectors along an isofrequency contour in cortex are interconnected with the same isofrequency contours in the MGB.

Processing is presumably being accomplished within these complex divergent-convergent patterns of projections by combining auditory information in specific ways. It is of interest that the level of complexity of the divergent and convergent patterns of connections for the auditory system appears to be greater than for the divergent and convergent patterns of connections of thalamus with cortex for the visual and somatosensory systems (Merzenich et al., '77). For instance, a line of cells in the lateral geniculate nucleus (LGN) projects to a point in striate cortex. The conversion from simpler center-surround receptive field properties in the LGN to more complex receptive field properties in the striate cortex is presumably accomplished by this column-to-locus projection. That a sheet of neurons in the ventral division projects onto a locus in AI cortex indicates that an added spatial dimension is being utilized by the auditory system for some, as yet unknown, processing purpose.

The convergent and divergent pattern of connections allows the prediction of the form of projections to and from loci in the MGB. A relatively large locus located anywhere in the MGB gives and receives projections in a continuous fashion centered along isofrequency contours in AI or AAF. A smaller locus in the ventral division projects in a periodic, discontinuous fashion along an isofrequency contour in AI. Conversely, that locus receives heavier projections from the same patchy regions which are centered along the isofrequency contours in AI.

Possible segregation of binaural response properties by a parallel segregation of connections

Recently, Imig and Adrian ('78), Imig and Brugge ('78), and Middlebrooks et al. ('78) have shown that there is a segregation of two major binaural response classes in AI. This segregation takes the form of repeating slabs that are oriented approximately normal to the isofrequency contours (Middlebrooks et al., '78). The two basic binaural response classes are cells that are excited by stimulation of either ear (EE) and cells that are excited by the contralateral ear stimulation, and the contralateral excitatory response is inhibited by simultaneous stimulation of the ipsilateral ear (EI).

These current studies are consistent with the existence of repeating subunits in both the MGB and AI. The fact that large AI cortical injections produce a continuous sheet of label in Vl, whereas small injections produce banding, suggests that there are repeating subunits in cortex that have alternating banding patterns of connection with Vl. It is possible that these repeating subunits are the EE and EI slabs. Thus, the banding in Vl may result from single small injections in cortex being restricted mostly to only one binaural response slab. This would suggest that Vl also contains binaural response slabs that are oriented normal to the isofrequency contours of Vl. Since there is also banding in the projection of AAF onto Vl, this observation suggests that there may also be a segregation of EE and EI neurons in AAF.

Interestingly, single injections of ^{3}H-l-leucine in the central nucleus of the inferior colliculus can result in a somewhat similar banded pattern of labelling in Vl (Andersen et al., '78). A segregation of binaural response

properties has been noted in the ICC by Roth et al. ('78). Thus, it is possible that there is a segregation in binaural response properties that passes in parallel and through a segregation of connections from the ICC through Vl to AI.

Although EE-EI segregation is a possible candidate, the actual functional significance of the banded segregation of connections between the ventral division and AI can only be determined through further study.

POl may be a subdivision of the MGB

Injections of tracers in AAF or AI produced thalamocortical and corticothalamic cell terminal arrays in the thalamus that were always continuous through POl into Dd. It has been noted that POl and Dd are very similar cytoarchitectonically (Rose and Woolsey, '58; Diamond et al., '69). In addition, POl contains predominantly sound-sensitive units with sharp tuning curves (Phillips and Irvine, '76). Thus, POl might properly be regarded as a subnucleus of the MGB.

Reciprocal structure of the thalamocortical and corticothalamic projections

These experiments demonstrate that all three cortical fields that were studied are reciprocally connected to the thalamus (with the reservations mentioned above). A reciprocity of thalamocortical connections has been sited extensively by previous investigators (see Ramón y Cajal, '03; Ades, '41; Diamond et al., '69; Colwell, '77). Reciprocal connections (in several species) between thalamus and cortex have been noted in the auditory system (see Rasmussen, '64; Diamond et al., '69; Horenstein and Yamamoto, '75; Colwell and Merzenich, '80), the visual system (see Jacobson and Trojanowski, '75; Colwell, '75; Ogren and Hendrickson, '76; Tigges et al., '77), and the somatosensory system (see Lin et al., '79; White and DeAmicis, '77). The current data and the studies of other sensory cortical fields cited above are consistent with the hypothesis that reciprocity of connectivity might be a general rule for connections between the dorsal thalamus and the cortex. The functional significance of these extraordinary complex reciprocal connections of the auditory forebrain demands further study.

ACKNOWLEDGMENTS

The authors would like to acknowledge Drs. Pat Patterson, Bill Crandall, and Russell Snyder, who participated in some of the experiments. We thank Ms. Mary Lui and Ms. Pat Clepper for their histological assistance and Ms. Anne-Christine Guerin, Ms. Mary H. Counselman, and Mr. Joe Molinari for their secretarial assistance. We thank Ms. Carol Andersen for proofreading the manuscript. Drs. Steven Cowell, Russell Snyder, John Middlebrooks, Marty Silverman, Linn Roth, Lindsay Aitkin, William Mehler, and Henry J. Ralston, III provided helpful advice and criticism. This research was supported by NIH grant NS-10414, Hearing Research, Inc., and the Coleman Fund.

LITERATURE CITED

Ades, H.W. (1941) Connections of the medial geniculate body in the cat. Arch. Neurol. Psychiat. *45:*138–144.

Aitkin, L.M. (1973) Medial geniculate body of the cat: Responses to tonal stimuli of neurons in medial division. J. Neurophysiol. *36:*275–283.

Aitkin, L.M., and W.R. Webster (1972) Medial geniculate body of the cat: Organization and responses to tonal stimuli of neurons in the ventral division. J. Neurophysiol. *35:*365–380.

Andersen, R.A., G.L. Roth, L.M. Aitkin, and M.M. Merzenich (1978) Organization of projection from the central nucleus of the inferior colliculus into the medial geniculate body of the cat. J. Acoust. Soc. Am. *64:*S65.

Andersen, R.A. (1979) Functional Connections of the Central Auditory Nervous System: Thalamocortical, Corticothalamic and Corticotectal Connections of the AI, AII, and AAF Auditory Cortical Fields. Thesis. University of California, San Francisco.

Brodal, A. (1969) Neurological Anatomy in Relation to Clinical Medicine. Oxford University Press, New York.

Casseday, J.H., I.T. Diamond, and J.K. Harting (1976) Auditory pathways to the cortex in *Tupaia glis*. J. Comp. Neurol. *166:*303–340.

Colwell, S.A. (1975) Thalamocortical-corticothalamic reciprocity: A combined anterograde-retrograde tracer study. Brain Res. *92:*443–449.

Colwell, S.A. (1977) Reciprocal Structure in the Medial Geniculate Body. Thesis, University of California, San Francisco.

Colwell, S.A., and M.M. Merzenich (1980) Corticothalamic projections from physiologically defined loci in AI of cat. (submitted.)

Cowan, W.M., D.I. Gottlieb, A.E. Hendrickson, J.L. Price, and T.A. Woolsey (1972) The autoradiographic demonstration of axonal connections in the central nervous system. Brain Res. *37:*21–51.

Cranford, J.L., S.J. Ladner, C.B.G. Campell, and W.D. Neff (1976) Efferent projections of the insular and temporal neocortex of the cat. Brain Res. *117:*195–210.

Diamond, I.T., K.L. Chow, and W.D. Neff (1958) Degeneration of caudal medial geniculate body following cortical lesion ventral to auditory area II in the cat. J. Comp. Neurol. *109:*349–362.

Diamond, I.T., E.G. Jones, T.P.S. Powell (1969) The projection of the auditory cortex upon the diencphalon and brainstem in the cat. Brain Res. *15:*305–340.

Diamond, I.T., and W.D. Neff (1957) Ablation of temporal cortex and discrimination of auditory patterns. J. Neurophysiol. *20:*300–315.

FitzPatrick, K.A., T.J. Imig, and R.A. Reale (1977) Thalamic projections to the posterior auditory field in cat. Society for Neuroscience Abstracts *3:*6.

Graham, R.C., and M.J. Karnovsky (1966) The early stages of absorption of injected horseradish peroxidase in the proximal tubules of the mouse kidney: Ultrastructural

cytochemistry by a new technique. J. Histochem. Cytochem. *14:*291–302.

Graybiel, A.M. (1973) The thalamo-cortical projection of the so-called posterior nuclear group: A study with anterograde degeneration methods in the cat. Brain Res. *49:*229–244.

Gross, N.B., W.S. Lifschitz, and D.J. Anderson (1974) Tonotopic organization of the auditory thalamus of the squirrel monkey *(Saimiri sciureus).* Brain Res. *65:*323–332.

Hanker, J.S., P.E. Yates., C.B. Metz, K.A. Carson, A. Light, and A. Rustioni (1977) A new specific, sensitive and noncarcinogenic reagent for the demonstration of horseradish peroxidase (HRP). Society for Neuroscience Abstracts *3:*30.

Hendrickson, A.E. (1972) Electron microscopic distribution of axoplasmic transport. J. Comp. Neurol. *144:*381–398.

Hind, J.E. (1953) An electrophysiological determination of tonotopic organization in auditory cortex of the cat. J. Neurophysiol. *16:*475–489.

Horenstein, S., and T. Yamamoto (1975) The relationship of the feline temporal cortex to the medial geniculate body. Society for Neuroscience Abstracts *1:*31.

Imig, T.J., and H.O. Adrian (1978) Binaural columns in the primary field (AI) of cat auditory cortex. Brain Res. *138:*241–257.

Imig, T.J., and J.F. Brugge (1978) Sources and terminations of callosal axons related to binaural and frequency maps in primary auditory cortex of the cat. J. Comp. Neurol. *182:*637–660.

Irvine, D.R.F. and H. Huebner (1979) Acoustic response characteristics of neurons in nonspecific areas of cat cerebral cortex. J. Neurophysiol. *42:*107–122.

Jacobson, S., and J.Q. Trojanowski (1975) Corticothalamic neurons and thalamocortical terminal fields, an investigation in rat using horseradish peroxidase and autoradiography. Brain Res. *85:*385–401.

Jones, E.G., and T.P.S. Powell (1971) An analysis of the posterior group of thalamic nuclei on the basis of its afferent connections. J. Comp. Neurol. *143:*185–216.

Kasama, T., K. Otani, and E. Kawana (1966) Projections of the motor, somatic sensory, auditory and visual cortices in cats. In: Correlative Neurosciences, T. Tokizane and J.P. Schade, eds. Elsevier, New York, vol. 21A, pp. 292–322.

Knight, P.A. (1977) Representation of the cochlea within the anterior auditory field (AAF) of the cat. Brain Res. *130:*447–467.

Kudo, M., and K. Niimi (1978) Ascending projections of the inferior colliculus onto the medial geniculate body in the cat studied by anterograde and retrograde tracing techniques. Brain Res. *155:*113–117.

LaVail, J.H., and M.J. LaVail (1972) Retrograde axonal transport in the central nervous system. Science *176:*1416–1417.

LaVail, J.H., K.R. Winston, and A. Tish (1973) A method based on retrograde axonal transport of protein for identification of cell bodies of origin of axons terminating within the CNS. Brain Res. *58:*470–477.

Lin, C., M.M. Merzenich, M. Sur, and J.H. Kaas (1979) Connections of areas 3b and 1 of the parietal somatosensory strip with the ventroposterior nucleus in the owl monkey *(Aotus Trivirgatus).* J. Comp. Neurol. *185:*355–372.

Locke, S. (1961) The projection of the magnocellular medial geniculate body. J. Comp. Neurol. *116:*179–194.

Merzenich, M.M., and M.D. Reid (1974) Representation of the cochlea within the inferior colliculus of the cat. Brain Res. *77:*397–415.

Merzenich, M.M., P.L. Knight, and G.L. Roth (1975) Representation of cochlea within primary auditory cortex in the cat. J. Neurophysiol. *38:*231–249.

Merzenich, M.M., G.L. Roth, R.A. Andersen, P.L. Knight, and S.A. Colwell (1977) Some basic features of organization of the central auditory system. In: Psychophysics and Physiology of Hearing, E.F. Evans and J.P. Wilson, eds. Academic Press, London,

Mettler, F.A. (1932) Connections of the auditory cortex in the cat. J. Comp. Neurol. *55:*139–183.

Middlebrooks, J.C., R.W. Dykes, and M.M. Merzenich (1978) Binaural response-specific bands within AI in the cat: Specialization within isofrequency contours. Society for Neuroscience Abstracts *4:*8.

Moore, R.Y., and J.M. Goldberg (1963) Ascending projections of the inferior colliculus in the cat. J. Comp. Neurol. *121:*109–136.

Morest, D.K. (1964) The neuronal architecture of the medial geniculate body of the cat. J. Anat. *99:*143–160.

Morest, D.K. (1965) The laminar structure of the medial geniculate body of the cat. J. Anat. *99:*143–160.

Neff, W.D., J.F. Fisher, I.T. Diamond, and M. Yela (1956) Role of auditory cortex in a discrimination requiring localization of sound in space. J. Neurophysiol. *16:*475–489.

Niimi, K., and F. Naito (1974) Cortical projections of the medial geniculate body in the cat. Exp. Brain Res. *19:*326–342.

Ogren, M., and A. Hendrickson (1976) Pathways between striate cortex and subcortical regions in *Macaca mulatta* and *Saimiri sciureus:* Evidence for a reciprocal pulvinar connection. Exp. Neurol. *53:*780–800.

Oliver, D.L., and W.C. Hall (1978) The medial geniculate body of the tree shrew, *Tupaia glis.* I. Cytoarchitecture and midbrain connections. J. Comp. Neurol. *182:*423–458.

Phillips, D.P., and D.R.F. Irvine (1976) Acoustic input to neurons in pulvinar-posterior complex of cat thalamus. Proc. Australian Physiol. Pharmacol. Soc. *7:*126P.

Pontes, C., F.F. Reis, and A. Sousa-Pinto (1975) The auditory cortical projections onto the medial geniculate body in the cat. An anatomical study with silver and autoradiographic methods. Brain Res. *91:*43–63.

Ralston, H.J. III, and P.V. Sharpe (1973) The identification of thalamocortical relay cells in the adult cat by means of retrograde axonal transport of horseradish peroxidase. Brain Res. *62:*273–278.

Ramón y Cajal, S. (1903) Las fibras nerviosas de origen cerebral del tuburculo cuadrigemino anterior y del talamo optico. Trab. Lab. Inv. Biol. *2:*5–20.

Ramón y Cajal, S. (1955) Histologie du Systeme Nerveux de L'home et des Vertebres. (Reprinted from the original 1909–1911 ed.) Consejo Superior de Investigaciones Cientificas, Madrid.

Rasmussen, G.L. (1964) Anatomic relationships of the ascending and descending auditory systems. In: Neurological Aspects of Auditory and Vestibular Disorders, W.S. Field and B.R. Alford, eds, C.C. Thomas, Springfield, Ill., pp. 5–19.

Rioch, D. (1929) Studies on the diencephalon of carnivora: The nuclear configuration of the thalamus, epithalamus, and hypothalamus of the dog and cat. J. Comp. Neurol. *49:*1–119.

Rose, J.E. (1949) The cellular structure of the auditory region of the cat. J. Comp. Neurol. *91:*409–440.

Rose, J.E., D.O. Greenwood, J.M. Goldberg, and J.E. Hind (1963) Some discharge characteristics of single neurons in the inferior colliculus of the cat. I. Tonotopic organization, relation of spike-counts to tone intensity, and firing patterns of single elements. J. Neurophysiol. *26:*294–320.

Rose, J.E., and C.N. Woolsey (1949) The relations of the thalamic connections, cellular structure and evocable electrical activity in the auditory region of the cat. J. Comp. Neurol. *91:*441–466.

Rose, J.E., and C.N. Woolsey (1958) Cortical connections and functional organization of the thalamic auditory system of the cat. In: Biological and Biochemical Bases of Behavior, H.F. Harlow and C.N. Woolsey, eds. University of Wisconsin Press, Madison, pp. 127–150.

Roth, G.L. (1977) Some Features of the Anatomical and Physiological Organization of the Central Nucleus of the Inferior Colliculus: Implications for its Role in the Processing of Auditory Information. Thesis, University of California, San Francisco.

Roth, G.L., L.M. Aitkin, R.A. Andersen, and M.M. Merzenich (1978) Some features of the spatial organization of the central nucleus of the inferior colliculus of the cat. J. Comp. Neurol. *182:*661–680.

Sousa-Pinto, A. (1973) Cortical projections of the medial geniculate body in the cat. Adv. Anat. Embryol. Cell Biol. *48:*1–42.

Tigges, J., M. Tigges, and A.A. Perachio (1977) Complementary laminar terminations of afferents to Area 17 originating in Area 18 and in the lateral geniculate nucleus in squirrel monkey. J. Comp. Neurol. *176:*87–100.

Trojanowski, J.Q., and S. Jacobson (1975) A combined horseradish peroxidase-autoradiographic investigation of reciprocal connections between superior temporal gyrus and pulvinar in squirrel monkey. Brain Res. *85:*347–353.

Tunturi, A.R. (1950) Physiological determination of the arrangement of the afferent connections to the middle ectosylvian area in the dog. Am. J. Physiol. *162:*489–502.

Van Noort, J. (1969) The Structure and Connections of the Inferior Colliculus. van Gorcum, Assen.

Waller, W.H. (1940) Thalamic degeneration induced by temporal lesions in the cat. J. Anat. *74:*528–536.

White, E.L., and R.A. DeAmicis (1977) Afferent and efferent projections of the region in mouse Sml cortex which contains the posteromedial barrel subfield. J. Comp. Neurol. *175:*455–482.

Wilson, M.E., and B.G. Cragg (1969) Projection from the medial geniculate body to the cerebral cortex of the cat. Brain Res. *13:*462–475.

Winer, J.A., I.T. Diamond, and D. Raczkowski (1977) Subdivisions of the auditory cortex of the cat: The retrograde transport of horseradish peroxidase to the medial geniculate body and posterior thalamic nuclei. J. Comp. Neurol. *176:*387–418.

Wong-Riley, M.T.T. (1976) Endogenous peroxidatic activity in brain stem neurons as demonstrated by their staining with diaminobenzidine in normal squirrel monkeys. Brain Res. *108:*257–277.

Woollard, H.H. and J.A. Harpman (1939) The cortical projection of the medial geniculate body. J. of Neur. and Psychiat. *2:*35–44.

Woolsey, C.N. (1960) Organization of cortical auditory system: A review and a synthesis. In: Neural Mechanisms of the Auditory and Vestibular Systems, G. Rasmussen and W. Windle, eds. Charles C. Thomas, Springfield, Ill., pp. 165–180.

Woolsey, C.N., and E.M. Walzl (1942) Topical projections of nerve fibers from local regions of the cochlea to the cerebral cortex of the cat. Bull. Johns Hopkins Hosp. *71:*315–344.